REGULATION OF HUNTINGTIN LOCALIZATION BY HMGB1

HMGB1 REGULATES THE NUCLEAR IMPORT OF HUNTINGTIN IN A ROS-DEPENDENT MANNER

By SUSIE SON, B.Sc. (Honours)

A Thesis Submitted to the School of Graduate Studies in Partial Fulfillment of the Requirements for the Degree Master of Science

McMaster University © Copyright by Susie Son, July 2017.

McMaster University MASTER OF SCIENCE (2017)
Hamilton, Ontario
(Biochemistry and Biomedical Sciences)

TITLE: HMGB1 regulates the nuclear import of huntingtin in a ROS-dependent manner
AUTHOR: Susie Son, B.Sc. (McMaster University)
SUPERVISOR: Dr. Ray Truant
NUMBER OF PAGES: 91

ABSTRACT

In healthy cells, huntingtin is primarily found in the cytoplasm; however, upon cellular stress, huntingtin is phosphorylated (phospho-huntingtin) at serines 13 and 16 of the amino-terminal N17 domain and shuttled into the nucleus. Such dynamism in nucleocytoplasmic translocation and post-translational modification suggests an important role for huntingtin in Huntington's disease (HD) pathogenesis as these phenotypes propose possible mechanisms for disease progression. Huntingtin nuclear import is also facilitated by its proline-tyrosine nuclear localization signal (PY-NLS), which harbours a highly conserved intervening sequence specific to the huntingtin gene. This encouraged a proteome investigation to identify potential protein partners of the PY-NLS. Results of this study revealed that high mobility group box 1 (HMGB1), a cofactor of base excision repair, uniquely bound to the wild-type PY-NLS, but not the PY-NLS KK177/178AA mutant. Immunofluorescence microscopy in human telomerase reverse transcriptase (hTERT) immortalized fibroblast cells using HMGB1- and phospho-huntingtin-specific antibodies revealed a promising association between the two, as changes in nuclear levels of HMGB1 positively correlated with nuclear levels of phospho-huntingtin. This relationship was further confirmed by co-immunoprecipitation of HMGB1 by the PY-NLS and N17 domain. Also, when exogenous oxidative stress was introduced, increased interaction between HMGB1 and huntingtin was observed. This suggests that HMGB1 facilitates the nuclear import of huntingtin in a ROS-dependent manner, and thus, presents a novel avenue to a potential therapeutic target in HD pathogenesis.

ACKNOWLEDGEMENTS

Thank you from the bottom of my heart to everyone who made this story possible.

I want to begin by sincerely thanking my supervisor, Dr. Ray Truant, for your continuous support throughout my journey and for inspiring me with knowledge and endless curiosity. Your passion for research was what convinced me to pursue this degree! I would also like to thank my committee members Dr. Kristin Hope and Dr. Karun Singh for all your invaluable insights and words of encouragement. Without your guidance, none of this would have been possible!

I also want to extend my purest thanks to past and present Truant lab members. Each day was filled with so much more happiness, excitement, and laughter because of your presence. I will forever cherish the friendships we have built and the memories we have created together. Claudia Hung, Laura Bowie, Laura DiGiovanni, Andrew Mocle, Glenn Walpole, Rohan Philip, Dr. Tam Maiuri, Mina Falcone, Jianrun Xia, and Sid Nath thank you so much for sharing your precious time with me to help me and teach me all the best of being a scientist!

Thank you to my family for being my guiding star and source of strength. Mom and dad, who have been and will always be my steadfast supporters and James, for being the best brother a sister can ask for! Thank you for being the bright light at the end of the tunnel.

And lastly, thank you Olivia Byun, my trusty partner in crime. No words can express and no act of gratitude can relay what your love and friendship means to me!

TABLE OF CONTENTS

ABSTRACT **4**

ACKNOWLEDGEMENTS **5**

TABLE OF CONTENTS **6**

FIGURE LIST **9**

ABBREVIATIONS **10**

DECLARATION OF ACADEMIC ACHIEVEMENT **12**

CHAPTER 1.0: INTRODUCTION **13**

1.1 Huntington's disease *14*

1.1.1 Diagnosis and neuropathology 14

1.1.2 The genetics of Huntington's disease 15

1.2 The huntingtin protein *16*

1.2.1 Huntingtin structure 16

1.2.2 Huntingtin localization 18

1.2.3 Huntingtin N17 domain and phosphorylation 19

1.2.4 Role of huntingtin in DNA damage repair 20

1.3 High mobility group box 1 (HMGB1) protein *21*

1.3.1 Structure and function 21

1.3.2 Localization patterns of HMGB1 and cell stress response 22

1.3.3 Role of HMGB1 in DNA damage repair 23

1.3.4 HMGB1 regulation of apoptosis and autophagy 24

1.4 HMGB1 inhibitors *25*

1.4.1 Glycyrrhizic acid (GA) 25

1.4.2 Epigallocatechin-3-gallate (EGCG) 25

1.4.3 Tanshinone IIA (TIIA) 26

1.4.4 Ethyl pyruvate (EP) 26

1.5 Clinical potential of HMGB1 ..... *27*

1.6 Thesis rationale *28*

CHAPTER 2.0: EXPERIMENTAL PROCEDURES..... 30

2.1 Tissue culture..... 31

2.2 Antibodies..... 31

2.3 Plasmid constructs..... 32

2.4 Oligonucleotides..... 32

2.5 Transfection..... 33

2.6 Immunofluorescence..... 33

2.7 Microscopy..... 34

2.8 Peptide affinity chromatography..... 34

2.9 Co-immunoprecipitation and western blot analysis..... 35

2.10 Pearson correlation and nuclear intensity quantification..... 36

2.11 Statistics..... 37

CHAPTER 3.0: RESULTS..... 38

3.1 HMGB1 binds to the huntingtin PY-NLS and its unique IVS..... 39

3.2 HMGB1 co-localizes with nuclear phospho-huntingtin with high correlation..... 40

3.3 HMGB1 binds to the huntingtin N17 domain..... 41

3.4 HMGB1 binding to the N17 domain is structure and charge-dependent..... 42

3.5 Full-length HMGB1 is required for binding..... 43

3.6 Oxidative stress increases the interaction between huntingtin and HMGB1..... 45

3.7 Residues involved in huntingtin phosphorylation are required for binding..... 46

3.8 Knockdown of HMGB1 greatly reduces nuclear phospho-huntingtin levels..... 47

CHAPTER 4.0: DISCUSSION..... 49

4.1 HMGB1 may be regulating huntingtin activity during DNA damage repair..... 50

4.2 HMGB1 is required for viability..... 51

4.3 The highly conserved IVS of huntingtin PY-NLS posits an important function..... 52

4.4 The p53-HMGB1 complex in the context of huntingtin biology..... 53

4.5 HMGB1 may be acting as a bridge between huntingtin PY-NLS and the N17 domain..... 54

CHAPTER 5.0: ADDITIONAL DATA..... 56

5.1 Glycyrrhizic acid and HMGB1..... 57

5.1.1 Fixation method is important in visualizing HMGB1 and huntingtin..... 57
5.1.2 Glycyrrhizic acid and huntingtin and HMGB1 localization..... 58
5.1.3 Investigating other HMGB1 inhibitors..... 59
5.1.4 Effects of GA under oxidative stress: Future work..... 59
5.2 HMGB1 and huntingtin in the context of DNA damage repair..... 60
5.2.1 Phospho-huntingtin and HMGB1 co-localize to sites of DNA damage..... 60
5.2.2 Localization of HMGB1 to euchromatin upon $KBrO_3$..... 61

CHAPTER 6.0: IMMEDIATE FUTURE DIRECTIONS..... 63
6.1 Additions to the N17 mutagenesis assay..... 64
6.2 Using FLIM-FRET to determine whether huntingtin and HMGB1 experience a direct interaction..... 65
6.3 Identifying important residues within the IVS..... 66
6.4 Huntingtin IVS as a potential NES..... 66
6.5 HMGB1 may be functioning as a karyopherin adaptor protein..... 67

CHAPTER 7.0: CONCLUSION..... 69

CHAPTER 8.0: FIGURES..... 71

REFERENCES..... 81

FIGURE LIST

Figure 1: The structure of the huntingtin protein.....17

Figure 2: The structure and sequence of the HMGB1 protein.....22

Figure 3: HMGB1 binds to the huntingtin PY-NLS and unique IVS.....72

Figure 4: Visualization and quantification of the correlation between huntingtin and HMGB1 localization.....73

Figure 5: HMGB1 co-immunoprecipitated with the N17 domain.....74

Figure 6: Huntingtin interacts with full-length HMGB1, but not its individual boxes.....75

Figure 7: Overexpression of HMGB1 boxes promotes cytoplasmic targeting of endogenous HMGB1.....75

Figure 8: The interaction between HMGB1 and huntingtin increases with oxidative stress.....76

Figure 9: HMGB1 knockdown abrogates nuclear entry of phospho-huntingtin.....77

Figure 10: Huntingtin localization in the presence of glycyrrhizic acid.....78

Figure 11: Localization of phosphorylated huntingtin and HMGB1 to sites of DNA damage via laser stripe assay.....79

Figure 12: The localization of HMGB1 to sites of euchromatin.....80

ABBREVIATIONS

Φ	Phi; hydrophobic amino acids
3-NP	3-nitropropionic acid
APE1	Apurinic/apyrimidinic endonuclease 1
ATM	Ataxia-telangiectasia mutated
BAC	Bacterial artificial chromosome
Bcl2	B-cell lymphoma 2
BER	Base excision repair
CAG	Cytosine-adenine-guanine
CD spectrometry	Circular dichroism spectrometry
Co-IP	Co-immunoprecipitation
CRM1	Chromosome region maintenance 1
CSK	Cytoskeleton
DMEM	Dulbecco's modified Eagle's medium
DNA	Deoxyribonucleic acid
DTT	Dithiothreitol
ECL	Electrochemiluminescence
EDTA	Ethylenediamine tetraacetic acid
EGCG	Epigallocatechin-3-gallate
EGTA	Ethylene glycol tetraacetic acid
EP	Ethyl pyruvate
EPR5526	Antibody specific to residues 1-100 of human huntingtin
ER	Endoplasmic reticulum
eYFP	Enhanced yellow fluorescent protein
FBS	Fetal bovine serum
FEN1	Flap endonuclease 1
FLIM	Fluorescent lifetime imaging microscopy
FRET	Föster resonance energy transfer
GA	Glycyrrhizic acid
GFP	Green fluorescent protein
GST	Glutathione S-transferase
IF	Immunofluorescence
IT15	Interesting transcript 15
IVS	Intervening sequence
HBSS	Hank's balanced salt solution
HD	Huntington's disease
HEAT	Huntingtin, Elongation factor 3, Protein Phosphatases 2A, mTOR
HMGB1	High mobility group box 1
HRP	Horse radish peroxidase

hTERT	Human telomerase reverse transcriptase
Htt	Huntingtin
HTT	Huntingtin gene
Kapα	Karyopherin alpha
Kapβ1	Karyopherin beta1
Kapβ2	Karyopherin beta2
$KBrO_3$	Potassium bromate
LepB	Leptomycin B
M8	Methionine 8
mab2166	Antibody specific to amino acids 181-810 of huntingtin
mCh	Monomeric cherry
MEM	Minimal essential medium
mRNA	Messenger ribonucleic acid
N17	The amino-terminal 17 amino acids of huntingtin
NES	Nuclear export signal
NLS	Nuclear localization signal
NMDA	N-methyl-D-aspartate receptor
NP40	Nonidet-P40
p53	Tumor suppressor involved in apoptosis
PACSIN1	Protein kinase C and casein kinase 2 substrate in neurons 1
PBS	Phosphate buffered saline
PCR	Polymerase chain reaction
PFA	Paraformaldehyde
Phospho-huntingtin	Phosphorylated huntingtin at amino acids 13 and 16
pN17	Phosphorylated N17
PTM	Post-translational modification
PVDF	Polyvinylidene fluoride
PY-NLS	Proline tyrosine nuclear localization signal
ROS	Reactive oxygen species
RPE1	Retinal pigment epithelial
SDS-PAGE	Sodium dodecyl sulfate polyacrylamide gel electrophoresis
shRNA	Short hairpin ribonucleic acid
ST*Hdh*	Transformed striatal progenitor cells from humanized exon1 knock-in mice
TBST	Tris buffered saline with tween-20
TIIA	Tanshinone IIA
TruHD	Patient-derived fibroblast cell line
WT	Wild-type
YAC	Yeast artificial chromosome

DECLARATION OF ACADEMIC ACHIEVEMENT

All experimental content within this thesis is the work of the author, Susie Son, except for the following:

Dr. Carly Desmond performed the peptide affinity chromatography experiment and generated the data for Figure 3B.

CHAPTER 1.0

INTRODUCTION

1.1 Huntington's disease

1.1.1 Diagnosis and neuropathology

Huntington's disease (HD) is an autosomal dominant disorder first identified in 1872 by an American physician named George Huntington (1). It is a neurodegenerative disease affecting as many as 1 in 5,500 individuals, and is characterized by the clinical triad: disordered motor control, impaired cognition, and development of psychiatric disorders, particularly depression (2–4). Although HD itself is not fatal, patients often succumb to symptomatic complications, making pneumonia and heart disease the leading causes of mortality in HD patients (5). Due to the devastating psychiatric symptoms in HD, suicide is also prevalent (6). Unfortunately, there are no known cures or effective therapies for this disease at this time.

HD is a late-age onset disease where patients are generally diagnosed during their fourth decade of life (1). However, juvenile cases are also prevalent within about 12% of diseased individuals being children as young as two years old (7). As the disease progresses, neurodegeneration is most prominently found in the striatum, particularly in the medium spiny neurons, caudate nucleus, and putamen (8, 9). During later years, significant tissue loss is observed in the cerebral cortex, thalamus, and cerebellum (10). The majority of the cognitive and psychiatric symptoms of HD are likely caused by degeneration of the basal ganglia, since this region is crucial for learning new tasks and processing emotions (11).

1.1.2 The genetics of Huntington's disease

Since HD is transmitted in an autosomal dominant fashion, both males and females are equally vulnerable and only one copy of the mutant allele is required for disease acquisition. In 1993, the gene responsible for HD was identified as the *IT15* (interesting transcript 15) or *HTT* gene, located on the short arm of chromosome 4 (12). This gene codes for huntingtin, the protein responsible for HD when mutated, and possesses a characteristic sequence of cytosine-adenine-guanine (CAG) repeats, which encodes a polyglutamine tract. In healthy individuals, the CAG expansion is typically 6 to 36 repeats in length (Fig. 1B) (13). HD is fully penetrant when these CAG repeats unstably expand to greater than 40 repeats (mean length is at 43 CAG repeats), while reduced penetrance is common when lengths are between 37-40 (14). In fact, the age of disease onset is inversely proportional with the length of the polyglutamine tract, such that individuals with a longer CAG expansion manifest HD symptoms at an earlier age (15). However, genetic modifiers and environmental factors play a significant role in HD pathogenesis. For example, polymorphisms within genetic modifiers can either negatively or positively impact the expression of certain genes, which can greatly alter the disease progression of one patient compared to another (16). Although the underlying disease cannot be prevented, environmental factors that promote a healthy lifestyle, such as exercising, support networks, and reducing stress, are associated with later age of onset and better symptom management (17).

1.2 The huntingtin protein

1.2.1 Huntingtin structure

Huntingtin is a large, 350kDa protein that is ubiquitously expressed in all cells of the body (18). For many years, the structure of huntingtin remained a mystery; however, using imaging reconstruction via electron microscopy, it was identified that the huntingtin sequence was dominantly comprised of HEAT (Huntingtin, Elongation factor 3, Protein Phosphatases 2A, mTOR) repeats, which are domains involved in protein-protein interactions and scaffolding (19). They are made up of helix-turn-helix motifs of approximately 40 amino acids that form a larger solenoid structure when repeated and stacked. This provides a high degree of flexibility and allows the protein to actively modify its structure into a myriad of conformations (20, 21). As a result, proteins possessing HEAT repeats are more adaptable to mechanical stress and accessible to interaction domains of neighbouring proteins.

The most frequently characterized region of huntingtin is at its amino-terminal, particularly its unique exon1. This exon consists of three functionally essential domains: (1) the N17 domain, which encompasses the first 17 amino acids of the protein; (2) the polyglutamine tract that determines the onset of HD; and (3) the proline-rich region, which consists of two stretches of 11 and 10 proline residues separated by a proline-rich intervening sequence (Fig. 1) (22). Using circular dichroism (CD) spectroscopy and X-ray crystallography, the N17 domain was determined to form an amphipathic alpha-helix until it reaches the polyglutamine tract, where the secondary structure is lost and

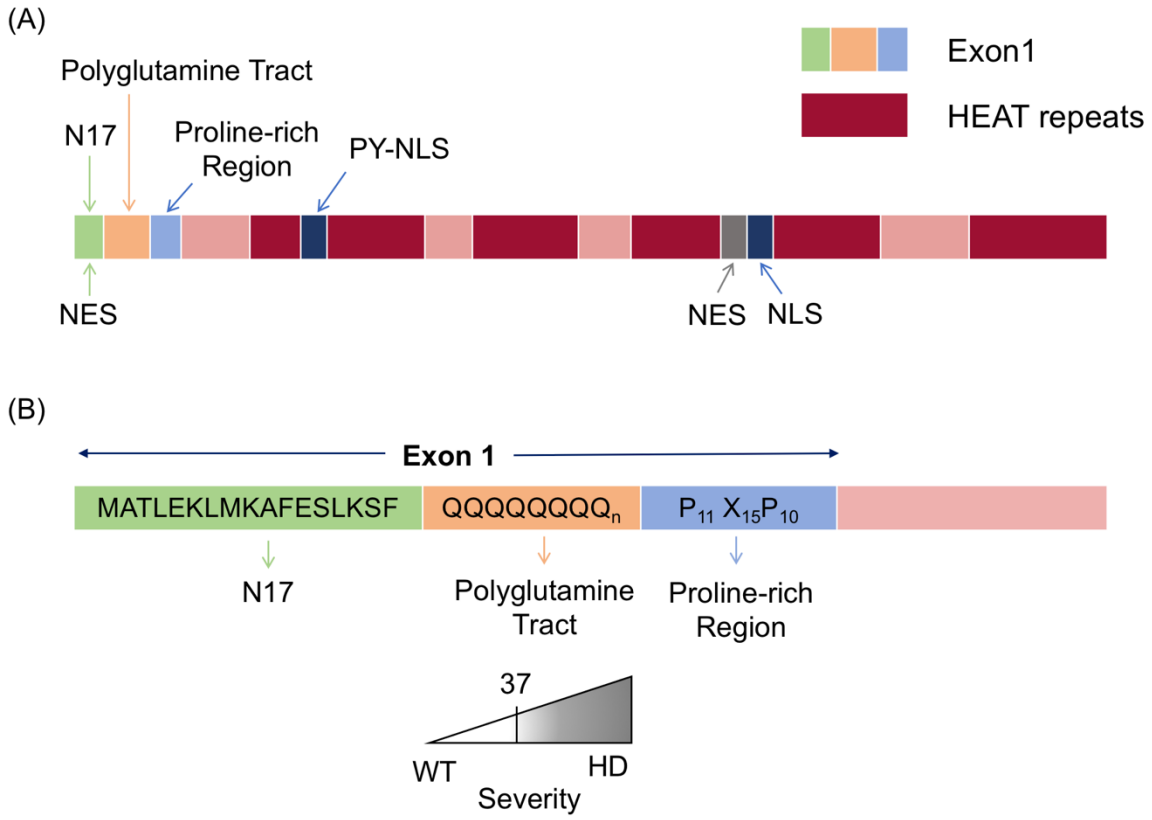

Figure 1: *The structure of the huntingtin protein.* (A) The huntingtin protein is approximately 350kDa in size and 3144 amino acids in length. It is made up of HEAT repeats (maroon), two NLSs (navy blue), two NESs (gray, green; the N17 sequence is a CRM1-dependent NES), and a conserved exon1 (green, orange, blue). (B) Exon1 is made up of three parts, the N17 domain (green), which is the first 17 amino acids at the amino-terminus, the polyglutamine tract (orange), and the proline-rich region (blue). Schematic is not to scale. A monotone gradient, indicating the degree of severity in HD, is included below the sequence of exon1. In HD the age of disease onset is inversely proportional with the length of the polyglutamine tract, such that individuals with a longer CAG expansion, exceeding 37 repeats, manifest HD symptoms at an earlier age.

remains as a random coil (23). The first proline-rich repeat was also found to adopt a helical form, but again loses its structure at the beginning of the mixed proline intervening sequence (23). Although conflicting data have been reported, most

literature findings suggest that the polyglutamine domain becomes more structured as repeat lengths reach pathogenic range, alternating between random coils and beta-sheets (24).

1.2.2 Huntingtin localization

In healthy neurons, huntingtin is predominantly cytoplasmic, where it localizes to the endoplasmic reticulum (ER) and Golgi, as well as endocytic, lysosomal, and plasma membranes (22, 25, 26). However, when exposed to cellular stressors such as reactive oxygen species (ROS), nuclear entry of huntingtin is observed (22, 27). In HD, the neurons of the basal ganglia, particularly the striatum, and the cerebral cortex are most heavily affected by neurodegeneration caused by the toxic nuclear accumulation of mutant huntingtin (28). Nuclear entry of huntingtin is facilitated by a non-classical, proline-tyrosine nuclear localization signal (PY-NLS) located between amino acids 174-207 (29). Within this sequence exists a unique and structured region flanked by the three consensus epitopes of the PY-NLS, which are the basic charged region, a downstream conserved arginine, and a proline-tyrosine (PY) sequence. This region is called the 'intervening sequence' (IVS), and consists of 18 residues that are almost 100% conserved and exists only in the huntingtin gene in all species. The IVS is required for recognition by import proteins, karyopherin β1 and β2 (29).

Recently, we demonstrated that the huntingtin N17 domain is a ROS sensor, regulating huntingtin phosphorylation and localization. We have identified this sensor to

be the highly conserved methionine at position 8 (M8) of N17 (30). In response to ROS stress, M8 becomes oxidized which dissociates N17 from the ER membrane (31). This biochemical shift increases the solubility of N17 and induces its phosphorylation and nuclear retention.

1.2.3 Huntingtin N17 domain and phosphorylation

Huntingtin, particularly within its N17 domain, is known to experience various post-translational modifications (PTM) including phosphorylation, acetylation, sumoylation, and ubiquitination (32–34). Amongst this list, N17 phosphorylation (pN17) at serine 13 and serine 16 (S13 and S16 respectively) has been shown to be of greatest clinical interest due to various studies that suggest its capabilities in modifying HD pathogenesis (35, 36). This event is responsible for regulating the nuclear export signal (NES) function of N17 by inhibiting interaction with chromosome region maintenance 1 (CRM1) (37). In the context of mutant huntingtin, which carries an expanded polyglutamine tract, S13 and S16 are hypo-phosphorylated and restoration of this phosphorylation status changes the conformation of the protein (32, 38). Clinical applications of N17 phosphorylation can be seen using phospho-mimetic aspartic acid mutations of N17. In BACHD mice, addition of pN17 was shown to abolish disease pathogenesis, and in YAC128 mice, intraventricular infusion of ganglioside GM1, which induces N17 phosphorylation, was shown to attenuate mutant huntingtin toxicity and restore normal motor functions (35, 36). As a result of such profound effects of pN17 in

HD pathology, studying its influences and identifying factors that promote this PTM is a promising future avenue to pursue for developing a treatment for HD.

1.2.4 Role of huntingtin in DNA damage repair

Huntingtin and its role in DNA damage repair is one of our major research foci. By immunofluorescence, we observed the co-localization of phosphorylated huntingtin at sites of DNA damage with key proteins such as: (1) p53, a transcriptional factor known to participate in various cell stress response signals including DNA damage, oxidative stress, and apoptosis; (2) ataxia-telangiectasia mutated (ATM) kinase that is activated by double stranded DNA breaks and oxidative stress; and (3) other DNA damage repair machinery, such as apurinic/apyrimidinic endonuclease 1 (APE1) and flap endonuclease 1 (FEN1) (39–42).

Furthermore, studies have shown that somatic expansion of the polyglutamine tract of mutant huntingtin is dependent on the base excision repair of oxidized DNA (43). These studies implicate oxidative DNA damage in HD pathology and suggest a potential role of huntingtin in DNA damage repair. The co-localization of phosphorylated huntingtin, the PTM achieved upon stress, with DNA damage machinery further suggests that these proteins may be interacting with each other to functionally cooperate in the repair process.

1.3. High mobility group box 1 (HMGB1) protein

1.3.1 Structure and function

HMGB1 is a member of the high mobility group box (HMGB) family within the high mobility group (HMG) superfamily (44). This family was first isolated in the 1970s as abundant, heterogeneous, non-histone components of chromatin, and were named after their high electrophoretic mobility in polyacrylamide gels and solubility in 2-5% trichloroacetic acid (44, 45). HMGB1 is a small nuclear 30kDa protein that is ubiquitously expressed (46). It is defined by its three domains, two of which, box A (residues 1-79) and box B (residues 88-162), are known to bind to chromatin and bend DNA (Fig. 2A) (47–50). They have a characteristic L-shaped fold created by three alpha-helices that are structurally and sequentially similar and fairly conserved (51). The third domain of HMGB1 is an acidic tail, which is known to function as a protein-protein interaction domain and is comprised of a mixture of 30 glutamic acid and aspartic acid residues (52).

HMGB1 is a chromatin-binding factor and inflammatory agent known to be multifaceted in function and concomitant in a diverse array of cellular systems, such as base excision repair (BER), autophagy, apoptosis, and inflammatory and oxidative stress response (53–55). Although HMGB1 is predominantly nuclear, it is also found in the cytoplasm and extracellular matrix where it functions as a signaling molecule during inflammation, cell differentiation and migration, wound healing, and tumour progression (56, 57).

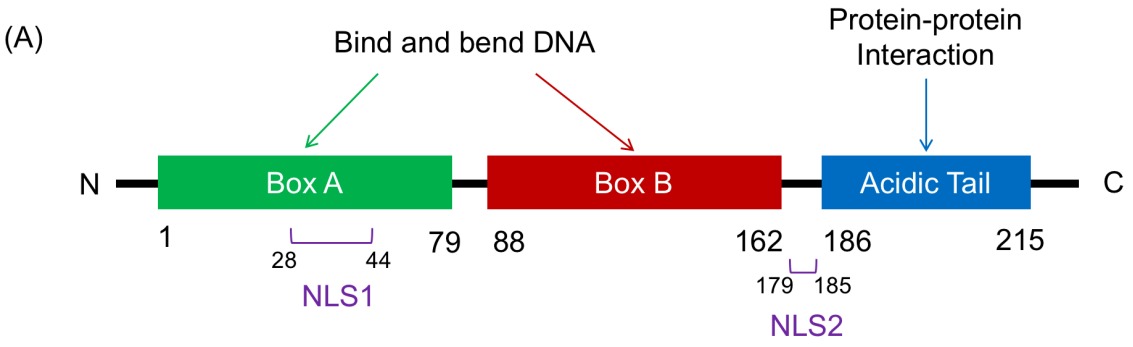

(B)

MGKGDPKKPRGKMSSYAFFVQTCREEHKKKHPDASVNFSEFSKKCSERWKTMSA
KEKGKFEDMAKADKARYEREMKTYIPPKGETKKKFKDPNAPKRPPSAFFLFCSE
YRPKIKGEHPGLSIGDVAKKLGEMWNNTAADDKQPYEKKAAKLKEKYEKDIAAY
RAKGKPDAAKKGVVKAEKSKKKKEEEEDEEDEEDEEEEEDEEDEDEEEDDDDD

Figure 2: *The structure and sequence of the HMGB1 protein.* (A) HMGB1 is a small protein of approximately 30kDa. It is 215 amino acids in length and contains 3 domains. The first two are box A (green, aa 1-79) and B (red, aa 88-162), which are responsible for binding to chromatin to bend and distort DNA. They are structurally homologous. The final domain is the acidic tail (blue, aa 186-215), which is responsible for protein-protein interactions. (B) This is the sequence of HMGB1 where residues for box A are in green, box B are in red, and the acidic tail are in blue. Black residues are the linker regions between adjacent domains. Also, there are two NLSs located between amino acids 28-44 and 179-185 (purple and bolded). All the basic residues have been underlined.

1.3.2 Localization patterns of HMGB1 and cell stress response

When cells are stressed, particularly by oxidizing agents, it has been frequently reported in literature that HMGB1 translocates to the cytoplasm (58). This localization is likely achieved by two NLSs within the HMGB1 sequence at amino acid positions 28-44 and 179-185, and potentially two non-classical NESs (the locations of these NESs remain ambiguous), which are believed to be CRM1-dependent signals (59, 60). When both NLSs are post-translationally modified, either through acetylation or phosphorylation,

HMGB1 is shuttled into the cytoplasm, which ultimately leads to its secretion into the extracellular matrix (59). It is important to note that both NLSs must undergo this modification in order to achieve nuclear export and prevent the re-entry of HMGB1 back into the nucleus.

1.3.3 Role of HMGB1 in DNA damage repair

HMGB1 is a known co-factor in BER (46). It binds to cruciforms, DNA breaks, and minor grooves of the DNA without sequence specificity, and is capable of introducing bends and kinks into linear DNA (61, 62). The architectural role of HMGB1 in the assembly of nucleoprotein complexes is highly conserved across species (63, 64). A study performed by Prasad *et al.* validated this function by using mass spectrometry to characterize HMGB1 as a protein specifically interacting with the BER intermediate. Purified HMGB1 was then found to stimulate APE1 and FEN1 activity on BER substrates, such as DNA polymerase β, which is responsible for removing deoxyribose phosphate during BER (65). Further investigation of the role of HMGB1 in BER led to the discovery that HMGB1 accumulates at sites of oxidative DNA damage in living cells. Conducted by Prasad *et al.*, this phenotype was observed using a laser stripe assay, a method for tracking the localization of proteins to damaged DNA. This represents a promising avenue for further exploration not only in HMGB1 biology, but in the overall DNA damage repair pathway.

1.3.4 HMGB1 regulation of apoptosis and autophagy

Cell viability is regulated by the balance between apoptosis and autophagy. Apoptosis is the process by which damaged, aged, ectopic, or mutated cells are eliminated, while autophagy is the process by which cell maintenance takes place via the recycling of proteins using the lysosomal degradation pathway (66–68). Since the regulation of cell fate is crucial to its survival, there are various proteins and cell signals involved in the crosstalk between these two pathways, for example HMGB1 (69, 70). Cytosolic HMGB1 is an important player in autophagy in that it binds to Beclin 1, an interactor of several cofactors to regulate the lipid kinase Vps-35 protein and induce autophagy (71, 72). When this interaction occurs, HMGB1 competes with Bcl2, an inhibitor of autophagy, for binding to allow Beclin 1 to carry out its functions (58). HMGB1 also forms a complex with p53, a tumor suppressor known to promote apoptosis, in the nucleus to facilitate its nucleocytoplasmic shuttling (70). This interaction is essential for proper maintenance of the cell because in the absence of p53, levels of free-floating HMGB1 are elevated, and greater amounts of HMGB1-Beclin 1 complexes are formed. This promotes autophagy and inhibits apoptosis. However, when HMGB1 is removed from the system, Bcl2 is free to bind to Beclin 1, and accumulation of p53 is observed. This results in hyperactivation of apoptosis and prevention of autophagy. Therefore, proper stoichiometric levels of HMGB1 are required to ensure correct cell fate determination.

1.4. HMGB1 inhibitors

1.4.1 Glycyrrhizic acid (GA)

Glycyrrhizic acid (GA), also known as glycyrrhizin or glycyrrhizinic acid, is the sweet-tasting constituent of *Glycyrrhiza glabra*, which is the scientific name for licorice root (73). This compound is an anti-inflammatory drug that inhibits the chemoattractant and mitogenic activities of HMGB1 (74). NMR and fluorescence studies indicate that GA binds to HMGB1 directly at the two shallow concave surfaces formed by the arms of box A and B, at a dissociation constant (K_d) of ~150 μM. Furthermore, GA has previously been used in many clinical applications. For example, in Japan and China, GA is commonly administered at high doses to hepatitis B and C patients (75). The outcomes of this treatment are satisfactory with few side effects and low toxicity.

1.4.2 Epigallocatechin-3-gallate (EGCG)

Epigallocatechin-3-gallate (EGCG) is a major component of *Camellia sinensis*, also known as green tea (76). Studies have demonstrated that it has several health benefits in diseases that are linked to oxidative stress, atherosclerosis, cancer, and cardiovascular disease (57, 77–79). With respect to HMGB1, EGCG is commonly known as an HMGB1 inhibitor that stimulates autophagy and reduces cytoplasmic HMGB1 levels in endotoxin-stimulated macrophages (76). EGCG also prevents clustering of exogenous HMGB1 on macrophage cell surfaces that are responsible for HMGB1-mediated inflammatory responses (80). Additionally, EGCG is implicated in HD by inhibiting the

aggregation of mutant huntingtin exon1 protein in a dose-dependent manner (81). Ehrnhoefer *et al.* elucidated this relationship by observing improvement in motor function and reduction in photoreceptor degeneration in HD flies overexpressing mutant huntingtin. These results suggested that modulators of huntingtin exon1 misfolding and oligomerization, such as EGCG, were likely to reduce polyglutamine-mediated toxicity *in vivo*.

1.4.3 Tanshinone IIA (TIIA)

Tanshinone IIA (TIIA) is a steroid derivative classified as a pigment extracted from a Chinese herb called Danshen, often referred to as red sage (82). This HMGB1 inhibitor stimulates internalization of exogenous HMGB1 into macrophage cytoplasmic vesicles, which delivers them to vacuoles for degradation (80). TIIA also inhibits acetylcholinesterase, which is an enzyme involved in eliminating the HMGB1-inhibiting neurotransmitter, acetylcholine (83). As of now, there are no known functions or mechanisms that connect TIIA to HD or the huntingtin protein.

1.4.4 Ethyl Pyruvate (EP)

Ethyl pyruvate (EP) is a simple derivative of the endogenous metabolite, pyruvic acid, and is an HMGB1 inhibitor commonly known to prevent the nucleocytoplasmic translocation of HMGB1 (83, 84). EP has been implicated in treatments for cancer, sepsis, and chronic colitis, suggesting that it may have some importance in studies

pertaining to therapeutic targeting (85, 86). Moreover, EP also displays a positive function in HD pathogenesis. Experimentation using an HD mouse model demonstrated that EP can be a potential neuroprotective molecule for promoting survival in striatal neurons that have been treated with 3-nitropropionic acid (3-NP), an inhibitor of mitochondrial complex II (87). This observation suggests a promising path for future studies.

1.5. Clinical potential of HMGB1

HMGB1 has been implicated in therapeutic remedies for various diseases. For example, it has appeared in clinical trials specific to treatments for sepsis, prostate cancer, cutaneous malignancies, autoimmunity, and cardiac disease (88–92). This may be due to its involvement in a plethora of pathways as a multifunctional protein. HMGB1 acts as a cofactor for BER and an architectural protein for DNA attachment and modification, making it an attractive subject for clinical investigations pertaining to DNA damage-related diseases. Furthermore, its identity as a proinflammatory cytokine suggests that it could be a valid drug target in disorders associated with inflammation and cell signaling. Now, we seek to apply our knowledge of HMGB1 and huntingtin to elucidate its potential in HD therapy.

1.6. Thesis rationale

The relationship between huntingtin and HMGB1 was first investigated by Dr. Carly Desmond, a previous PhD student. During her thesis, she discovered a short sequence within the proline-tyrosine nuclear localization signal (PY-NLS) of huntingtin, called the intervening sequence (IVS). To broaden the characterization of this NLS, and potentially the IVS, she conducted a proteomics analysis of ST*Hdh*$^{Q7/Q7}$ cell lysates via mass spectrometry to identify possible protein interaction partners. A list of the top interacting proteins was compiled and further filtered using peptide affinity chromatography. From this list, she identified one protein that exclusively interacted with the wild-type PY-NLS peptide, but not with its mutant, PY-NLS KK177/178AA. This protein was high mobility group box 1 (HMGB1).

This finding posited a potential relationship between huntingtin and HMGB1, because HMGB1 is a known cofactor of BER, which coincides with one of our recently reported findings – that huntingtin is recruited to sites of DNA damage. This connection presents the possibility that the interaction between HMGB1 and huntingtin may play a significant role in understanding their functions in the context of DNA damage repair.

Furthermore, the relevance of studying HMGB1 in the context of huntingtin localization was also encouraged by the results of a natural compound library screen conducted by Laura Bowie, a PhD candidate in the lab. In this screen, a compound was categorized as a hit when a phenotypic difference in endogenous phosphorylated huntingtin, stained with the phosphorylated N17 (pN17) antibody, was detected using

an unbiased, principal component analysis tool known as PhenoRipper (93). Amongst her hits, we identified glycyrrhizic acid (GA), which is the most recognized inhibitor of HMGB1 cytokine function (80).

Thus, my thesis was initiated upon the discovery that HMGB1 specifically bound to the huntingtin PY-NLS, and that HMGB1 inhibitors may influence huntingtin PTMs.

CHAPTER 2.0

EXPERIMENTAL PROCEDURES

2.1 Tissue culture

T-antigen immortalized, wild-type mouse striatal ST*Hdh*$^{Q7/Q7}$ cells (kind gift from M.E. MacDonald, MGH) were cultured in Dulbecco's modified Eagle's medium (DMEM) with 10% fetal bovine serum (FBS) at 33^{o}C with 5% CO_2. hTERT-immortalized retinal pigment epithelial cells (RPE1) (ATCC) were grown in DMEM/F12 1:1 media with 10% FBS, 0.26% $NaHCO_3$ (Bioshop), and 0.01mg/mL hygromycin B (Invitrogen) at 37 ^{o}C with 5% CO_2. hTERT-immortalized wild-type TruHD-Q21Q18 and HD mutant TruHD-Q43Q17 patient-derived fibroblast cells (Hung et al., manuscript in preparation) were cultured in minimal essential medium (MEM) with 15% FBS and 1% GlutaMax at 37 ^{o}C with 5% CO_2. All media and supplements were from Life Technologies unless stated otherwise.

2.2 Antibodies

The following primary antibodies were used in this study: anti-HMGB1 rabbit polyclonal, anti-huntingtin EPR5526, anti-GFP (Abcam); and anti-HMGB1 mouse monoclonal (Abnova). Huntingtin phosphorylation was detected using a previously characterized and validated antibody against huntingtin S13 and S16 phospho epitopes of the N17 domain (anti-pN17) (32). The antibody specific for unmodified huntingtin at the N17 domain (anti-N17) was also characterized and validated (32). Secondary antibodies against rabbit, mouse, and goat IgG, directly conjugated to Alexa Fluor 488, 594, or Cy5 (Invitrogen) were used for immunofluorescence and anti-rabbit IgG and anti-

mouse IgG horse radish peroxidase (HRP) conjugates (Abcam) were used for western blot analysis.

2.3 Plasmid constructs

Double-stranded synthetic DNA oligonucleotides (Integrated DNA Technologies) encoding the PY-NLS and IVS sequence of huntingtin containing BspEI and Acc65I overhangs were cloned between BspE1/Acc65I sites of peYFPN1 (BD Biosciences/Clontech) to generate Htt PY-NLS-eYFPN1 and Htt IVS-eYFPN1 plasmids. Additional huntingtin plasmids of wild-type N17 and its mutants (E5AE12A, K6AK9A, M8L, M8P, S13A, S16A) were created as previously described (30, 32). HMGB1 fragments (box A and box B) were generated by first amplifying the gene via PCR from plasmid mCh-HMGB1 using oligonucleotides specified below. The PCR product was cleaved with BspEI and Acc65I and subcloned into BspEI/Acc65I sites of peYFPN1. All DNA manipulation enzymes and buffers were purchased from New England Biolabs. All plasmid constructs were verified by nucleotide sequencing (McMaster MOBIX facility).

2.4 Oligonucleotides

PCR amplicons were generated from plasmid mCh-HMGB1 using oligonucleotides with BspEI and Acc65I overhangs. The following constructs were created using their respective forward and reverse primers:

HMGB1 Box A-peYFP (Forward primer: AGTCtccggaATGGGCAAAGGAGATCC; Reverse primer: GATCggtaccGATATAGGTTTTCATTTCTCT)

HMGB1 Box B-peYFP (Forward primer: AGTCtccggaGTTCAAGGATCCCAATGC; Reverse primer: CATGggtaccATATGCAGCAATATCCTTTTC)

2.5 Transfection

ST*Hdh*$^{Q7/Q7}$ cells were transfected using TransIT-X2 (Mirus) and treated or imaged approximately 24h after transfection. For knockdown, a human HMGB1 shRNA cocktail of four unique 29mer in a retroviral GFP vector (OriGene) was diluted in 1X Opti-MEM (Life Technologies) and transfected into RPE1 cells using TransIT-X2. The complex was incubated for approximately 72h prior to immunofluorescence analysis as described below.

2.6 Immunofluorescence

Cells were cultured on glass-bottom tissue culture dishes to approximately 80% confluence prior to treatment, and subsequently fixed using 4% (w/v) paraformaldehyde (PFA) (Millipore) in phosphate buffered saline (PBS) at room temperature for 20min. Cells were washed three times in PBS and permeabilized in 0.05% (v/v) Triton X-100 (Bioshop) at room temperature for 10min. Cells were thoroughly washed in PBS and blocked in antibody solution (2% FBS, 0.1% (v/v) Triton X-100 in 1X Tris-buffered saline) at room temperature for 10min. Primary antibodies were diluted 1:250-1:500 in

antibody solution and incubated on cells at 4^{o}C overnight prior to the addition of secondary antibodies diluted 1:250 in antibody solution at room temperature for 45min. Then, nuclei were stained using Hoechst dye 33258 (0.2μg/mL in PBS) (Life Technologies) at room temperature for 12min. Cells were thoroughly washed in PBS between each incubation step and imaged in PBS.

2.7 Microscopy

Confocal laser scanning microscopy was performed using the Nikon Eclipse Ti epifluorescence inverted microscope equipped with GaAsP detectors. Live and fixed cells were captured on the Nikon A1+ confocal system using the 405nm, 488nm, 561nm, and 640nm laser lines with a PLAN APO 60/1.4 oil objective and PLAN APO 20/0.75 dry objective. Image acquisition was completed using the Nikon NIS-Elements Advanced Research 4.30.02v 64-bit acquisition software (Nikon). Widefield epifluorescence microscopy was conducted on a Nikon Eclipse Ti inverted microscope using a PLAN APO 60/1.4 oil objective and Spectra X LED lamp (Lumencor) captured on an Orca-Flash 4.0 CMOS camera (Hamamatsu).

2.8 Peptide affinity chromatography

WT PY-NLS and KK177/178AA PY-NLS mutant peptides were diluted to a concentration of 1mg/mL in coupling buffer (50mM TRIS, 5mM EDTA-Na, pH 8.5), and coupled to resin as instructed by the manufacturer (Thermo Fisher). The resin was then

equilibrated in binding buffer (0.1M NaCl, 10mM HEPES pH 7.6, 10% (v/v) glycerol). ST*Hdh*$^{Q7/Q7}$ cell lysates were prepared in NP40 lysis buffer (0.15M NaCl, 0.05M TRIS pH 8, 1% (w/v) NP40) and diluted 1:2 in binding buffer. Samples were incubated for 1h rotating at 4^{o}C before loading into a pipette tip column stuffed with glass wool. Columns were washed four times with binding buffer and once in washing buffer (0.3M NaCl, 10mM HEPES pH 7.6, 10% (v/v) glycerol). Bound proteins were then eluted in 0.5M NaCl. All affinity chromatography was conducted at 4^{o}C and analyzed by western blot for the presence of HMGB1 as described below.

2.9 Co-immunoprecipitation and western blot analysis

ST*Hdh*$^{Q7/Q7}$ cells were transfected with YFP fusion proteins as outlined above. At 24h post transfection, cells were either treated with or without 10mM 3-nitropropionic acid (3-NP) (Sigma-Aldrich) for 1.5h in Hank's balanced salt solution (HBSS) (Life Technologies). Obtained cell pellets were re-suspended and incubated in 1% PFA at room temperature for 10min and then quenched in 125mM glycine (Bioshop) at room temperature for 5min. Cells were washed in ice cold PBS twice and lysed in cytoskeleton (CSK) lysis buffer (10mM PIPES, pH 6.8, 100mM NaCl, 300mM sucrose, 3mM $MgCl_2$, 1mM EGTA, 0.5% (v/v) Triton X-100) containing 1X protease and phosSTOP inhibitor cocktails (Roche) for 3min. Supernatants were pre-cleared in Protein A agarose beads (Sigma) rotating for 1h at 4^{o}C . Pre-cleared products were collected and incubated in fresh Protein A agarose beads with anti-GFP or anti-huntingtin EPR5526 for 2h rotating at 4^{o}C.

Samples were washed thoroughly in CSK lysis buffer and were denatured in 1X DTT+3X SDS loading dye (New England Biolabs) for 10min at 100^{o}C. Solubilized proteins and untreated precleared supernatants were resolved on a 4-12% SDS-polyacrylamide gradient gel (Bio-Rad) and electroblotted onto a PVDF membrane (Millipore). Membranes were treated in methanol for 8min and washed three times in TBST (50mM Tris-HCl, pH7.5, 150mM NaCl, 0.1% (v/v) Tween-20) for 10min each prior to blocking in TBST containing 5% (w/v) skim milk powder at room temperature for 2h. Membranes were then incubated with primary antibodies diluted 1:2500 in the same blocking buffer overnight at 4^{o}C. Membranes were washed six times in TBST+2.5% (w/v) milk prior to the incubation of secondary antibodies diluted at 1:50000 in blocking buffer at room temperature for 45min. Membranes were washed as previously described and visualized using ECL (Millipore) and Microchemi (DNR Bio-Imaging Systems). The Gel Analyzer functions on ImageJ 1.49v were used for densitometric analysis of western blots.

2.10 Pearson correlation and nuclear intensity quantification

TruHD-Q21Q18 and TruHD-Q43Q17 fibroblast cells were treated and fixed for immunofluorescence and widefield epifluorescence microscopy as outlined above. A homemade Python script written on PyCharm CE 2016.1.2 was used to calculate the correlation of nuclear intensity of pN17 and HMGB1. Raw, unprocessed images, captured at 16-bit depth, were thresholded using the intersect of the Hoechst stain and YFP (488nm) or far red (640nm) fluorescence to detect pN17 or endogenous HMGB1,

respectively. Images were separated via a morphological closing and connectivity-based segmentation and mean nuclear intensity was computed for each segmented region. Regions were excluded if their mean nuclear intensity was greater or less than two standard deviations from the mean for each image. Using Pearson's correlation coefficient, the correlation of mean nuclear intensity of pN17 and endogenous HMGB1 was calculated in approximately 500 cells from 3 trials. Results were displayed in a bar graph with standard error bars.

2.11 Statistics

All statistical analysis was completed using the Real Statistics Excel add-in (Microsoft). If data passed the Shapiro-Wilk normality test, statistical significance was determined using a Student's t-test. If data was not normal, the Mann-Whitney test was used.

CHAPTER 3.0

RESULTS

Our current model of huntingtin localization proposes that upon oxidative stress huntingtin becomes phosphorylated at its unique N17 domain and translocates into the nucleus (30). We also know that another mechanism of huntingtin nuclear import exists via the karyopherin β1/2-dependent PY-NLS (94). Since huntingtin is a large protein incapable of crossing the nuclear membrane alone, its movement is dependent on the activity of surrounding molecules, like kinases, and PTMs (32). To further understand huntingtin nuclear import and assisted translocation, a proteomics study was conducted to identify potential protein partners to the huntingtin PY-NLS. Preliminary mass spectrometry data suggests that high mobility group box 1 (HMGB1) may be uniquely binding to this region. Thus, we decided to investigate the interaction between huntingtin and HMGB1 to determine whether a relationship existed.

3.1 HMGB1 binds to the huntingtin PY-NLS and its unique IVS

The huntingtin PY-NLS contains a short intervening sequence (IVS) of 18 amino acids flanked by a proline on either terminus (Fig. 3A). Its sequence is highly conserved amongst all species and exists only within the huntingtin gene, making the IVS an extremely unique region. Peptide affinity chromatography was conducted to test the specificity of HMGB1 binding to the PY-NLS. Lysates of T-antigen immortalized mouse striatal (ST*Hdh*$^{Q7/Q7}$) cells were passed through either the wild-type or mutant KK177/178AA PY-NLS peptide-coupled columns. Western blotting the eluted products revealed that HMGB1 binds to the wild-type PY-NLS, but not its KK177/178AA mutant

(Fig. 3B). This suggests that the binding of HMGB1 to the huntingtin PY-NLS is specific, and that its basic epitope is required. To confirm this interaction, we performed a co-immunoprecipitation (Co-IP) assay using ST*Hdh*$^{Q7/Q7}$ cells transfected with a PY-NLS-YFP fluorescent fusion plasmid. Since the binding of HMGB1 to the PY-NLS may be a transient one, lysates were treated in 1% paraformaldehyde (PFA) prior to lysis to crosslink any existing interactions. Analysis by western immunoblotting revealed that the pull-down of endogenous HMGB1 by the huntingtin PY-NLS was successful (Fig. 3C).

Next, a Co-IP was performed using ST*Hdh*$^{Q7/Q7}$ cell lysates overexpressing IVS-YFP to determine whether the IVS alone was sufficient for HMGB1 binding, since the huntingtin IVS is highly conserved and unlike conventional IVSs. When the Co-IP products were immunoblotted with anti-HMGB1, the pull-down of HMGB1 by the IVS was confirmed by the presence of its protein band (Fig. 3C). This interaction strengthens the importance of the unique huntingtin IVS as this sequence alone is sufficient for HMGB1 binding.

3.2 HMGB1 co-localizes with nuclear phospho-huntingtin with high correlation

To establish the localization pattern of endogenous HMGB1 and huntingtin, TruHD-Q21Q18 (WT) and TruHD-Q43Q17 (HD) human fibroblast cells were fixed and co-stained with anti-HMGB1 and either anti-pN17 (probes phosphorylated N17 at S13 and S16) or anti-N17 (probes unmodified N17) antibodies. Under steady state conditions, HMGB1 was exclusively nuclear, as expected, while huntingtin was predominantly

cytoplasmic with varying levels of nuclear intensity, particularly of phospho-huntingtin (Fig. 4A). When nuclear fluorescence was quantified and analyzed using Pearson correlation, a high correlation between HMGB1 and phospho-huntingtin in both WT and HD lines was detected (Fig. 4B). Qualitative analysis suggested a complementary relationship where greater nuclear phospho-huntingtin was observed in nuclei when there was high HMGB1 intensity, and less when there was low HMGB1 intensity. This pattern was unique to phospho-huntingtin and absent in its unmodified counterpart as indicated by its significantly reduced correlation value. This led us to hypothesize that HMGB1 may be regulating the nuclear translocation of phospho-huntingtin. Also, since modification of huntingtin by phosphorylation is prevalent under oxidative stress, this observation suggested that the relationship between HMGB1 and huntingtin may be ROS-dependent.

3.3 HMGB1 binds to the huntingtin N17 domain

We have previously reported that nuclear translocation of huntingtin is achieved by phosphorylation of the N17 domain (22). If HMGB1 binds to the PY-NLS to regulate its function, we then inquired whether a similar relationship could be seen with the N17 domain. To address this question, a Co-IP was conducted in ST*Hdh*$^{Q7/Q7}$ cells stably expressing the N17-YFP fluorescent fusion peptide. Proteins that were immunoprecipitated by N17-YFP were separated by SDS-PAGE and blotted using anti-HMGB1. All trials included both positive and negative controls and the membranes were

stripped and reprobed for N17-YFP to rule out the possibility of non-specific binding. Western blot analysis indicated the presence of endogenous HMGB1 in the Co-IP product and thus, the interaction between HMGB1 and the N17 domain (Fig. 5A).

This experiment was repeated using wild-type ST*Hdh*$^{Q7/Q7}$ cells transfected with fluorescently-tagged N17-YFP peptide to confirm this binding relationship via a secondary approach. Using the same Co-IP procedure, pull down of HMGB1 by N17-YFP was observed (Fig. 5B). Not only does this suggest that HMGB1 has a binding affinity for N17, but it also implies that it is a member of the huntingtin interactome.

3.4 HMGB1 binding to the N17 domain is structure and charge-dependent

To further characterize this interaction, we endeavoured to identify the binding region between HMGB1 and N17 by performing a mutagenesis assay. N17 mutants were selected based on their ability to disrupt the charge and structure of the peptide. Since HMGB1 is a small protein, made up of two basic boxes and an acidic tail, we wanted to test the importance of the charged residues required for electrostatic binding (Fig. 2B). The N17 E5AE12A acidic mutant was used to observe whether the acidic residues of N17 interacted with the basic residues of either, or both, box A or B. Next, the N17 K6AK9A basic mutant was used to test the binding of basic N17 residues to the acidic tail. Co-IP experiments in ST*Hdh*$^{Q7/Q7}$ cells were conducted to quantify the amount of HMGB1 immunoprecipitated by each of the overexpressed N17 mutants. Interestingly, a dramatic reduction in HMGB1 binding was observed in all cases, suggesting that

achieving the correct charge is important for binding (Fig. 5C). Furthermore, there is a significant twofold reduction in the binding ability of the N17 K6AK9A basic mutant in comparison to the N17 E5AE12A acidic mutant, indicating that the interaction may be more dependent on its basic residues for binding to the acidic tail.

Next, we executed a Co-IP assay using an N17 proline mutant at methionine 8 (M8P) to assess the consequences of disrupting the structure. Since the N17 peptide is an amphipathic alpha-helix where its charged residues, E5, E12, K6, and K9, are aligned against one face, we hypothesized that the correct structure is required for proper electrostatic binding to occur. To verify our postulation, ST*Hdh*$^{Q7/Q7}$ cells overexpressing N17 M8P-YFP were lysed and prepared for Co-IP. When anti-HMGB1 was immunoblotted to quantify its binding affinity for the structural mutant of N17, a markedly reduced amount of HMGB1 was measured (Fig. 5C). This suggests that the structure of the N17 peptide is crucial for proper alignment of its charged residues and further facilitation of its interaction with HMGB1.

3.5 Full-length HMGB1 is required for binding

HMGB1 is a multifunctional protein implicated in several key pathways throughout the cell. One of its well-characterized roles is its identity in the nucleus as a cofactor for BER. This function is mainly executed by boxes A and B of HMGB1, which are known for their ability to interact and distort DNA. Also, our team recently elucidated a novel role for huntingtin as a scaffolding protein in the ATM oxidative DNA damage

response complex (39). By integrating the role of the HMGB1 boxes and our knowledge of huntingtin in DNA damage repair, we decided to explore the binding affinity of each individual box to the N17 domain and examine if either box was sufficient for binding. Prior to conducting a Co-IP assay, each box, as well as full-length HMGB1, were cloned into a YFP vector to create fluorescent fusion proteins. The resulting box A-YFP, box B-YFP, and HMGB1-YFP were overexpressed in ST*Hdh*$^{Q7/Q7}$ cells to perform Co-IP experiments and assess if there was an interaction with endogenous full-length huntingtin. Upon immunostaining using anti-HMGB1, no HMGB1 was detected in the Co-IP products of both box A and B, but was clearly evident in the HMGB1-YFP blot (Fig. 6). This indicated that the interaction between huntingtin and HMGB1 is applicable only in the context of full-length HMGB1 and that individual HMGB1 boxes are insufficient for binding.

To determine whether a characteristic phenotype could be identified, an immunofluorescence experiment was conducted to visualize the localization pattern of phospho-huntingtin in the presence of HMGB1 fragments. This qualitative approach was performed by individually overexpressing box A-YFP and box B-YFP, and co-staining for endogenous HMGB1 and phospho-huntingtin. Although the localization of phospho-huntingtin appeared unchanged, it was evident that the nuclear export of HMGB1 took place by its presence in the cytoplasm (Fig. 7). This observation suggests that HMGB1 boxes may be competing with endogenous huntingtin for binding with HMGB1. Perhaps

HMGB1 boxes are regulating the cytoplasmic translocation of full-length HMGB1, which ultimately disrupts or delays its interaction with endogenous huntingtin.

3.6 Oxidative stress increases the interaction between huntingtin and HMGB1

We have recently reported a novel function of huntingtin as a ROS sensor, regulating its phosphorylation and localization. To further this characterization, we decided to explore the relationship between huntingtin and HMGB1 in the presence of intracellular ROS. Co-IP assays were conducted in the same manner as previously described in the ST*Hdh*$^{Q7/Q7}$ line stably expressing N17-YFP. Cells were either dosed with or without 3-nitropropionic acid (3-NP), a mitochondrial complex II inhibitor that induces accumulation of ROS, to recapitulate an intracellular environment undergoing oxidative stress (95). Upon treatment with 3-NP, there was a significant increase in the amount of HMGB1 co-immunoprecipitated by N17, suggesting that this interaction is dependent on ROS levels (Fig. 8A,B).

This observation was further supported by co-immunoprecipitation of HMGB1 with full-length huntingtin. Since we have established that the interaction of HMGB1 with N17 is increased upon ROS stress, we wanted to confirm whether this relationship was translatable to the context of endogenous full-length huntingtin at proper stoichiometric levels. Thus, in lieu of probing for fluorescent fusion proteins, anti-huntingtin EPR5526, an antibody specific to residues 1-100 of human huntingtin, was used to detect endogenous levels of this protein. The Co-IP product was subsequently

separated and blotted for the presence of HMGB1. When the membrane was immunoblotted with anti-HMGB1, an even greater increase in the amount of binding was noted (Fig. 8C,D). Interestingly, the amount of HMGB1 interacting with endogenous huntingtin was multiplied by five times in the presence of 3-NP, while a twofold increase was seen using exogenous N17-YFP. This difference indicated that the interaction between HMGB1 and huntingtin was much more sensitive at proper stoichiometric levels.

To visualize this relationship, an immunofluorescence (IF) assay was conducted in ST*Hdh*$^{Q7/Q7}$ cells by overexpressing N17-YFP and probing for endogenous HMGB1. We see that under normal physiological conditions, N17-YFP is cytoplasmic, predominantly localized in the ER, and HMGB1 is nuclear, as expected. However, upon 3-NP treatment, the nuclear import of N17-YFP is noted, while a portion of HMGB1 translocates to the cytoplasm (Fig. 8E). This active change in localization corresponds with similar observations reported in literature, which also validates the credibility of our system (96). This result also demonstrates co-localization of nuclear HMGB1 and nuclear N17, which further supports the idea that upon oxidative stress the interaction between HMGB1 and the N17 domain is increased.

3.7 Residues involved in huntingtin phosphorylation are required for binding

Now that we have established that ROS stress increases the binding of HMGB1 and huntingtin, we sought to investigate how this interaction occurred. Again, a

mutagenesis assay was performed using N17 mutants to confirm that oxidation and phosphorylation are required for binding. First, to test the importance of oxidation, a previously validated N17 M8L mutant was selected, since M8 becomes oxidized by ROS to promote phosphorylation and this mutant prevents this oxidation event. Next, N17 S13A and S16A mutants were used, since phosphorylation occurs at S13 and S16. Each mutant was tagged with the YFP fluorophore in preparation for Co-IP and overexpressed in ST*Hdh*$^{Q7/Q7}$ prior to 3-NP treatment. When each Co-IP product was processed and quantified, we observed a drastic reduction in binding in all cases, as well as no significant difference in these levels even after the induction of oxidative stress by 3-NP (Fig. 8B). This suggests that the interaction of HMGB1 with the N17 domain is not only dependent on charge and structure, but also on the ability of N17 to be oxidized and phosphorylated. Furthermore, these residues, M8, S13, and S16, must be present in order to observe the robust increase in binding upon ROS stress.

3.8 Knockdown of HMGB1 greatly reduces nuclear phospho-huntingtin levels

We have shown that HMGB1 binds to two critical regions involved in huntingtin transport and that the nuclear levels of phospho-huntingtin are highly correlated with nuclear levels of HMGB1. Our next step was to assess this relationship in the context of the whole cellular system and test whether HMGB1 is required for the nuclear import of huntingtin. Thus, a knockdown assay was performed to reduce the expression of endogenous HMGB1 and then examine the localization pattern of phospho-huntingtin.

Knockdown was achieved in hTERT-immortalized retinal pigment epithelial (RPE1) cells using a human HMGB1 shRNA and was confirmed by the presence of a GFP fluorescent marker. When HMGB1 levels were reduced, there was near abolishment of nuclear phospho-huntingtin, as well as its characteristic, distinct nuclear puncta (Fig. 9). Not only was this consistent with our hypothesis, but also suggested that HMGB1 is required for the nuclear translocation of phospho-huntingtin.

CHAPTER 4.0

DISCUSSION

In this study, we have demonstrated the importance of HMGB1 in huntingtin biology. We have characterized HMGB1 as a ROS-dependent regulator of huntingtin nuclear import and validated this relationship using both qualitative and quantitative methods. We observed an increase in the magnitude of huntingtin-HMGB1 binding in the presence of ROS, and abrogation of huntingtin nuclear entry when HMGB1 was knocked down. We now know that HMGB1 is a member of the huntingtin interactome, binding to the PY-NLS and N17 domain. Both these regions are involved in huntingtin localization, which further supports our study of HMGB1 as a regulator of huntingtin localization.

4.1 HMGB1 may be regulating huntingtin activity during DNA damage repair

Since HMGB1 is a multifunctional protein, beyond its role as a regulator, there are various other pathways and mechanisms that have yet to be explored. For example, we have previously reported that HMGB1 co-localizes with phospho-huntingtin at sites of DNA damage using a laser stripe assay. Although this relationship was not pursued further, huntingtin, and its association with the DNA damage repair pathway and machinery, represents a promising foundation for future studies. HMGB1 is established for its ability to bind to linear DNA, loops, and cruciforms to manipulate DNA and as a cofactor in BER (61, 97). HMGB1 has been implicated in a diverse array of studies examining the activation and repression of DNA damage repair mechanisms and has been reported to have binding capabilities with proteins involved in these processes

(46). Currently, there are no known DNA binding motifs in huntingtin as it is predominantly comprised of HEAT repeats. This encourages us to hypothesize a novel function of HMGB1 as a stabilizer of huntingtin during DNA damage repair. When cells undergo oxidative stress, which induces DNA damage, HMGB1 may act as a bridge to tighten the proximity of huntingtin to damaged DNA. Since HMGB1 is a small protein of only 215 amino acids, it could secure huntingtin at these sites without markedly impeding its function in scaffolding DNA repair machinery. With further research into this aspect of HMGB1 and huntingtin biology, we postulate promising discoveries with regards to HD therapies associated with DNA damage.

4.2 HMGB1 is required for viability

HMGB1 is ubiquitously expressed throughout the body, and is highly conserved both structurally and sequentially throughout the animal kingdom, especially in mammals (98). This suggests that this protein serves an essential function within the cell and is required for life. In fact, it has been shown in mouse models that HMGB1 knockout newborns die within 24 hours (99). This may explain why, during a search for a human HMGB1 knockout cell line, we noticed that it was nearly impossible to find. Although HMGB1 was supposedly knocked out, protein was still detected via western blot analysis. We later realized that HMGB1 has various paralogs: HMGB2, HMGB3, and HMGB4 (100). Although HMGB3 and HMGB4 have minor variations in their domain lengths and sequence order, HMGB2 shares sequence similarity with HMGB1 of >80%,

and is almost identical in structure, charge, and functions in DNA binding and repair (101). However, beyond its association with DNA, HMGB2 is also known to participate in embryogenesis and the inflammatory response pathway, and is downregulated by p53 in disease, such as colorectal cancer (102–104). This raises a question as to whether some of the relationships identified between HMGB1 and huntingtin are also applicable to HMGB2. Further investigating HMGB2 and its potential involvement in huntingtin biology may open new doors to novel functions and capabilities of both proteins.

4.3 The highly conserved IVS of huntingtin PY-NLS posits an important function

The non-classical huntingtin PY-NLS harbours an IVS flanked between two prolines. This sequence is extremely unique, is nearly 100% conserved, and is found only in the huntingtin gene. This suggests that this region has been evolutionarily conserved for purposes that are still yet to be discovered. We have reported using a Co-IP assay that the IVS is sufficient for HMGB1 binding. Although this relationship was not further explored, the uniqueness of the IVS indicates that this interaction is important and efforts should be made to understand the purpose of it.

The huntingtin IVS is considered to be unlike other conventional 8-13 amino acid IVS regions due to its longer, 18 amino acid, length. Within the huntingtin IVS, there is also a hydrophobic sequence (LRAALWRFAEL) that closely aligns with the consensus of an NES ($\Phi X_{2\text{-}3}\Phi X_{2\text{-}3}\Phi X\Phi$) (Fig. 3A) (105). In fact, when in isolation, the IVS is observed to independently target the cytoplasm, suggesting a potential function in regulating the

activity of the huntingtin PY-NLS (29). Furthermore, the IVS is flanked on either side by proline residues and contains a rare tryptophan residue at its center. This is quite interesting as it coincides with the fact that HMGB1-binding motifs are generally short peptides that predominantly contain tryptophan and or proline (98). Investigating the huntingtin IVS as a potential HMGB1-binding motif can be one of many future directions to extend our understanding of the functions of this sequence in both huntingtin and HMGB1 activity.

4.4 The p53-HMGB1 complex in the context of huntingtin biology

HMGB1 forms a complex with tumor suppressor protein p53 to regulate the balance between autophagy and apoptosis (70). When HMGB1 is removed from the system, elevated levels of free-floating p53 drives the cell toward the apoptotic pathway. However, when greater than normal levels of HMGB1 are present, the cell fate is reversed to favour autophagy. Various studies have shown that HMGB1 facilitates DNA binding for a wide range of proteins, particularly transcription factors like p53 (106, 107). This may be done by manipulating the linear DNA into a more favourable conformation to facilitate greater access and binding, or by acting as a bridge to stabilize the position of a protein.

This knowledge can now be used to further understand huntingtin activity during apoptosis as early studies in HD identified a crucial interaction between mutant huntingtin and p53 (108). It has been demonstrated that within the huntingtin gene

there are multiple putative p53-responsive elements (40). p53-binding, both *in vitro* and *in vivo*, upregulates huntingtin mRNA and protein expression, suggesting that huntingtin activity is dependent on the behaviour of p53. We can extrapolate this relationship to the context of the whole cellular system by determining whether huntingtin is involved in regulating apoptosis and autophagy, and thus, cell fate determination. Not only will this elucidate the connection between HMGB1, p53, and huntingtin, but will also provide insights to disease mechanisms involving autophagy and apoptosis.

4.5 HMGB1 may be acting as a bridge between huntingtin PY-NLS and the N17 domain

In 2013, we reported a unique structural ability of huntingtin to fold back onto itself at downstream regions of the protein (38). Using Föster resonance energy transfer (FRET), we identified an intramolecular proximity between the N17 domain and the downstream proline-rich region of exon1. We demonstrated that the polyglutamine tract can act as a flexible hinge to allow interaction of the N17 domain with distal regions of huntingtin. Also, during this study, we described an interacting protein called protein kinase C and casein kinase 2 substrate in neurons 1 (PACSIN1) that has the ability to bind to both the N17 domain and the proline-rich region (109). PACSIN1 serves an important role in the cell by contributing to pathways responsible in the recycling of NMDA receptors and formation of neuronal spines (110, 111).

In this study, we have characterized similar binding capabilities in HMGB1 with the N17 domain and the PY-NLS at amino acids 174-207. Perhaps it is HMGB1, acting as

an interacting protein between the PY-NLS and N17 domain, that allows the regulation of huntingtin localization to take place. By facilitating crosstalk between these two regions, HMGB1 may be the key that is required for the nuclear entry of huntingtin. In the future, HMGB1 and its association with other regions of huntingtin can be explored to determine if it is required for the interaction of other domains, and the regulation of novel functions.

CHAPTER 5.0

ADDITIONAL DATA

5.1 Glycyrrhizic acid and HMGB1

The idea of investigating HMGB1 was first inspired by the results of a natural compound library screen conducted by Laura Bowie, a PhD candidate in the lab. Within this screen, a compound was categorized as a hit when a phenotypic difference in endogenous huntingtin stained with anti-pN17 was detected using an unbiased data profiling software known as PhenoRipper (93). One of her hits included a compound called glycyrrhizic acid (GA), which is a well-characterized inhibitor of HMGB1 cytokine and mitogenic function (74). Currently, there are no known functions of GA in the context of HMGB1 localization and huntingtin in general, thus a dose-response immunofluorescence assay was performed in mouse striatal (ST*Hdh*$^{Q7/Q7}$) cells to identify potential effects of GA on HMGB1 and huntingtin.

5.1.1 Fixation method is important in visualizing HMGB1 and huntingtin

Cells were first co-stained with anti-HMGB1 and anti-pN17, as this was the antibody used in the screen, to identify possible changes in HMGB1 and huntingtin localization when treated with varying concentrations of GA. Surprisingly, when the control cells were stained with anti-HMGB1, HMGB1 was cytoplasmic and localized to the endoplasmic reticulum (ER) (Fig. 10A). This was inconsistent with the literature and the well-known fact that wild-type HMGB1 is a very nuclear protein with little to no fluorescence within the cytoplasm (56).

After various rounds of troubleshooting, it was discovered that the cause of these contradicting results was fixation method-dependent. The unexpected outcome was the product of ice cold methanol fixation, since when cells were fixed using 4% paraformaldehyde (PFA), HMGB1 was nuclear and huntingtin was cytoplasmic, which were both the expected, control phenotypes (Fig. 10A). To capture representative data with proper HMGB1 and huntingtin localization using immunofluorescence, 4% PFA was used for all subsequent experiments. Although a follow up to this paradoxical result was not further pursued, it suggests that the relationship between HMGB1 and huntingtin may extend beyond the nucleus as they are both multifunctional proteins. Since HMGB1 was observed at the ER and since we know N17 is ER-bound under steady state conditions, we can postulate a secondary role occurring at this region (30).

5.1.2 Glycyrrhizic acid and huntingtin and HMGB1 localization

ST*Hdh*$^{Q7/Q7}$ cells were treated with GA in a dose-dependent manner and co-stained with anti-pN17. The GA concentration gradient was organized to include 0.5µM, 1µM (the concentration used in the screen), 2µM, 10µM, and 100µM. When analyzed using immunofluorescence microscopy, phospho-huntingtin was cytoplasmic regardless of GA concentration (Fig. 10B). We also used another huntingtin antibody, mab2166, which binds to an epitope located within amino acids 181-810 of huntingtin. When the same experiment was replicated using this antibody, huntingtin was also cytoplasmic at all concentrations (data not shown).

Although the results from Laura Bowie's screen were promising, the progress of this approach was placed on hold, since a robust change in huntingtin activity and localization could not be detected, despite fervent attempts.

5.1.3 Investigating other HMGB1 inhibitors

As a result of being a multifunctional protein, there are various known HMGB1 inhibitors, many of which are natural compounds. Thus, a number of HMGB1 inhibitors were examined to gain more insight on its activity, including tanshinone IIA (TIIA), epigallocatechin-3-gallate (EGCG), and ethyl pyruvate (EP). Cells were treated at varying concentrations of each compound (0.5µM to 100µM) and fixed with 4% PFA. Unfortunately, no noticeable difference in huntingtin or HMGB1 localization was detected, thus, further exploration using these compounds was not undertaken (data not shown). However, since further validation of the efficacy of these compounds was not pursued, the effects of TIIA, EGCG, and EP, remain inconclusive.

5.1.4 Effects of GA under oxidative stress: Future work

Now that we have established that HMGB1 regulates huntingtin localization in a ROS-dependent manner, perhaps future studies can investigate the effects of GA on HMGB1 and huntingtin localization in the presence of ROS stress. It would be interesting to see whether GA activity inhibits or further promotes this interaction, and whether an

unknown function of GA, otherwise dormant under steady state conditions, is uniquely activated upon oxidative stress.

5.2 HMGB1 and huntingtin in the context of DNA damage repair

We previously reported that huntingtin is a scaffolding protein in the ATM oxidative DNA damage response complex (39). Thus, by integrating the fact that HMGB1 is a co-factor in BER with the idea that phospho-huntingtin is found at sites of DNA damage, we hypothesized that HMGB1 will exhibit a synergistic relationship with huntingtin during DNA damage repair. Since there is no known DNA binding motif in huntingtin, as it is primarily made up of HEAT repeats, we postulated that HMGB1 plays an important role in stabilizing the position of huntingtin to allow it to complete its functions in DNA damage repair.

5.2.1 Phospho-huntingtin and HMGB1 co-localize to sites of DNA damage

A study conducted by Prasad *et al.* demonstrated that HMGB1 localizes to sites of DNA damage by performing a laser stripe assay, a technique used to induce DNA damage upon a region of interest in the nuclei of select cells (65). In order to confirm translocation of phospho-huntingtin and HMGB1 to areas of DNA damage, a laser stripe assay was executed in hTERT-immortalized human retinal epithelial (REP1) cells using a 405nm laser. Subsequent to the induction of DNA damage, cells were incubated for 5-20min, as this may be a time-sensitive procedure, and immediately fixed using 4% PFA.

After treatment, cells were probed with anti-pN17 and anti-HMGB1 antibodies to visualize the localization of these proteins. As expected, both HMGB1 and phospho-huntingtin accumulated at DNA damage-induced stripes (Fig. 11A). This active localization was seen at both 5 and 20min time points suggesting that this interaction occurs quickly and remains viable for some time.

Next, to determine whether HMGB1 was required for the localization of huntingtin to sites of DNA damage, the laser stripe assay was repeated after knocking down HMGB1 via shRNA transfection. When probed with anti-pN17, instead of observing a reduction in huntingtin at the stripe as we had expected, total huntingtin levels in the nucleus were reduced, if not, completely abolished (Fig. 11B). Although a robust difference in huntingtin levels at the stripe could not be seen subsequent to HMGB1 knockdown, the reduction of total huntingtin further supports the theory that nuclear levels of HMGB1 correlate with nuclear huntingtin.

5.2.2 Localization of HMGB1 to euchromatin upon $KBrO_3$ treatment

As an extension to our current understanding of huntingtin localization in the presence of oxidative stress, we wanted to simultaneously capture the movement of huntingtin and HMGB1 under these conditions. Live cell imaging was attempted in RPE1 cells co-transfected with mCh-HMGB1 and a camelid chromobody, tagged with a carboxy-terminal YFP and the SV40 NLS, capable of detecting endogenous huntingtin (39). Prior to imaging, cells were treated with 40mM $KBrO_3$ (potassium bromate) for 3h

to induce DNA damage. After approximately 2h, HMGB1 began to localize to areas that appeared like “holes”, which were regions that were not stained by Hoechst 33258 (Fig. 12). We postulated that these “holes” could either be nucleoli, or regions of euchromatin – loosely packed chromatin where there can be increased interaction with DNA. However, when we observed the activity of the huntingtin-bound chromobodies, we did not see co-localization with HMGB1. Although punctate regions began to form after 1.5h, they were unlike the bright, circular phospho-huntingtin puncta that we regularly observed. Nonetheless, changes were seen in both channels, suggesting that both HMGB1 and huntingtin are responding to oxidative damage in some manner.

CHAPTER 6.0:

IMMEDIATE FUTURE DIRECTIONS

6.1 Additions to the N17 mutagenesis assay

To further solidify the importance of N17 oxidation and phosphorylation in the binding of HMGB1 to huntingtin, there are three additional N17 mutants that can be included in our mutagenesis assay. In this study, N17 M8L-YFP was selected to represent the "reduced" form of M8 and to assess whether the abrogation of M8 sulfoxidation affected HMGB1 binding. Our results implicated that the oxidation of N17 is necessary because when a Co-IP assay was performed to test this relationship, HMGB1 binding with N17 M8L-YFP was significantly reduced. The M8L mutant does not; however, address the possibility that this reduction in binding was simply due to the change in residue and independent of N17 oxidation. Thus, N17 M8Q-YFP, an oxido-mimetic mutant, can be used to clarify this ambiguity. If the interaction was indeed dependent on the oxidation of N17, then HMGB1 binding to N17 should not be impeded by this mutant, since M8Q mimics M8 sulfoxidation.

Next, a similar Co-IP assay was conducted using phospho-resistant mutants, N17 S13A-YFP and N17 S16A-YFP, to demonstrate that HMGB1 binding was dependent on N17 phosphorylation. When the Co-IP products were quantified via western blotting, a significantly reduced amount of HMGB1 was detected, relative to the control. However, likewise to the M8L mutant, S13A and S16A do not clearly specify whether this reduction was due to the change in residue or because of the inhibition of N17 phosphorylation. Thus, phospho-mimetic mutants, N17 S13D-YFP and N17 S16D-YFP, can be used as a secondary method to confirm the phospho-dependence of HMGB1 binding. If the

phosphorylated state of N17 is necessary, then the amount of HMGB1 co-immunoprecipitated by the mutants can be expected to be like the N17-YFP control, since the aspartic acid of S13D and S16D mimic phospho-serine.

6.2 Using FLIM-FRET to determine whether huntingtin and HMGB1 experience a direct interaction

A study completed by Qi *et al.* demonstrated via a glutathione S-transferase (GST) pull-down assay that the acidic tail of HMGB1 directly interacts with mutant huntingtin, Htt^{Q111}, but not with wild-type huntingtin, Htt^{Q20} (112). This suggests that HMGB1 binds to huntingtin indirectly; however, to further confirm this interaction, we can employ Föster resonance energy transfer (FRET) to measure the closeness of these two proteins and fluorescent lifetime imaging microscopy (FLIM) to quantify it (113). If huntingtin and HMGB1 are indeed directly interacting, FRET will occur. This will be shown through the domination of the acceptor fluorophore in its emission spectrum and will be quantified using FLIM by indicating a decrease in fluorescence lifetime of the donor molecule (114). FRET is achieved when the following four conditions are met: (1) the donor and acceptor fluorophore must be in close spatial proximity of 10-100Å; (2) the emission spectrum of the donor must overlap with the excitation spectrum of the acceptor (ex. spectral overlap of YFP and mCerulean); (3) the dipole orientation of the donor and acceptor fluorophore must be parallel; and (4) the lifetime of the donor molecule must be of sufficient duration to allow FRET to occur (38). For this study, a

FLIM-FRET experiment can be initiated using a YFP fluorescent fusion peptide of an amino-terminal huntingtin or N17 fragment and mCerulean-HMGB1.

6.3 Identifying important residues within the IVS

As previously described, the huntingtin PY-NLS harbours an unconventional IVS that is 18 amino acids in length, almost 100% conserved in all species, and exists only within the huntingtin gene. Due to its uniqueness, we hypothesize that this region is important in the interaction of HMGB1 with huntingtin. In particular, there are a few residues within the IVS that can be targeted in a mutagenesis assay to look at the binding affinity of HMGB1 and the intracellular activity of huntingtin. Tryptophan (W190), arginine (R191), and phenylalanine (F192) are three possible residues. W190 may play a role in the interaction with HMGB1 as it is commonly observed in HMGB1-binding motifs, R191 is also an interesting amino acid since, if HMGB1 binding is charge-dependent, its position between two large and potentially important residues (W190 and F192) may be important, and F192, since its large side group may be responsible for interacting with the lipid membrane. Creating mutants of each and observing its nuclear localization and binding affinity to HMGB1 will be an informative experiment.

6.4 Huntingtin IVS as a potential NES

Since the IVS, in isolation, localizes to cytoplasmic vesicles and contains an NES consensus sequence, we reported a potential NES function within the IVS (Fig. 3A). A

Leptomycin B (LepB) experiment was conducted by Dr. Carly Desmond to determine whether this potential NES was CRM1-dependent, since LepB is an inhibitor of the nuclear export factor, CRM1 (115). Her results revealed no effect and change in localization, thus, the idea that the IVS may have a functional NES was dismissed. However, now that we have established that huntingtin activity and conformation is modified upon ROS stress, we propose that the IVS may also be sensitive to ROS. Thus, upon oxidative stress, we hypothesize that changes in huntingtin conformation or solubility may unmask the effects of LepB and inhibit the nuclear export of the IVS, suggesting that it contains a CRM1-dependent NES. To test this hypothesis, cells can be (1) transfected with an IVS fluorescent fusion peptide; (2) treated with 3-NP prior to the addition of LepB; (3) then fixed and prepared for immunofluorescence.

6.5 HMGB1 may be functioning as a karyopherin adaptor protein

In 2012, we published a paper describing the ability of the PY-NLS to utilize both the karyopherin β1 (Kapβ1) and karyopherin β2 (Kapβ2)-mediated import pathways to facilitate huntingtin nuclear entry (94). Proteins that use the Kapβ1 pathway require an adaptor protein, Kapα, that recognizes well-characterized, classical NLS consensus sequences consisting of either one (monopartite) or two (bipartite) basic-rich regions (116). Conversely, the Kapβ2-mediated pathway does not require an adapter protein and, in lieu of the classical NLS consensus, Kapβ2 recognizes the three epitopes of the non-classical PY-NLS. We identified that the PY-NLS activity can be mediated via both

Kapβ1 and β2 pathways by using human embryonic kidney (HEK293) cells, a cell line known to exhibit low nuclear import levels, despite the function of the PY-NLS. When either Kapβ1 or Kapβ2 was overexpressed, we observed that the PY-NLS activity in these cells was restored and that nuclear levels of huntingtin were increased. Interestingly, in HEK293 overexpressing Kapβ1, restoration of PY-NLS activity occurred without the need to overexpress the adaptor protein, Kapα. This suggested that, beyond its regulation via Kapβ2, the PY-NLS is also capable of using a Kapβ1-direct mechanism that is not the classical Kapα/β1 pathway.

However, now that we have established that HMGB1 regulates huntingtin localization, we hypothesize that the PY-NLS may in fact be utilizing the classical Kapα/β1 pathway where HMGB1 is functioning as the karyopherin adaptor protein. To test this theory, we can perform a Co-IP assay in the presence of ROS to identify whether Kapβ1 and or Kapβ2 are co-immunoprecipitated by endogenous huntingtin. HMGB1 can be immunoblotted as a control, where an increase in binding should be evident upon ROS stress. If HMGB1 is replacing the role of Kapα, then we postulate that levels of Kapβ1 will also increase in proportion with HMGB1. Thus, when a Co-IP is conducted, we expect to observe an increase in the levels of Kapβ1 and perhaps in Kapβ2, since the PY-NLS is also dependent on this pathway.

CHAPTER 7.0

CONCLUSION

The relationship between HMGB1 and huntingtin presents a number of avenues for promising discoveries. Recognizing that both huntingtin and HMGB1 are multifunctional proteins, we envision this investigation transforming into the progenitor of many more to come. We have reported that HMGB1 binds to the huntingtin PY-NLS at its basic epitope and highly conserved IVS. We have also shown that HMGB1 binds to the N17 domain, where we observed that structure and charge is important, and that this interaction is increased upon ROS stress. Using a knockdown assay, the importance of HMGB1 in huntingtin localization was validated by demonstrating that with dramatically reduced levels of HMGB1, nuclear phospho-huntingtin was also greatly reduced.

Now that we have established HMGB1 as a ROS-dependent regulator of huntingtin nuclear import, this study can be further extrapolated into the context of HD pathology. Ultimately, understanding HMGB1 in conjunction with huntingtin biology could play a paramount role in identifying potential drug targets and therapies for HD treatment.

CHAPTER 8.0

FIGURES

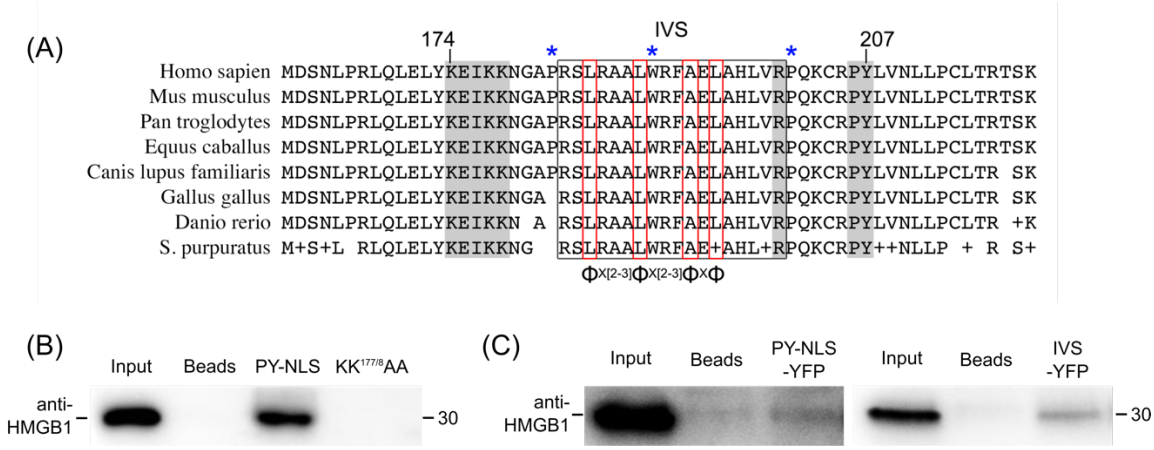

Figure 3: *HMGB1 binds to the huntingtin PY-NLS and unique IVS.* (A) The PY-NLS sequence is located between amino acids 174-207 and is characterized by three epitopes: the basic charged (KEIKK 174-178), arginine (R 200), and proline-tyrosine (PY 206-207), in gray. The 18 amino acid intervening sequence (IVS) is outlined in black. The red boxes outline hydrophobic residues that fit the NES consensus sequence (written below the alignment). Blue asterisks are used to indicate proline (P) and tryptophan (W) residues that may resemble an HMGB1-binding motif. This sequence alignment was adapted from Desmond *et al.* (29). (B) HMGB1 binds to the wild-type PY-NLS, but not the PY-NLS KK177/178AA mutant. This interaction was confirmed using peptide affinity chromatography. Bound proteins were eluted at 0.5M NaCl. (C) ST*Hdh*$^{Q7/Q7}$ cells were fixed in 1% PFA and lysed in CSK buffer. Lysates were incubated in protein A agarose beads with and without the YFP-specific antibody, anti-GFP. Co-IP products were separated by SDS-PAGE and immunoblotted with anti-HMGB1. The "Input" lane represents the positive control, the "Beads" lane represents the negative control, and lane three indicates the presence of HMGB1 co-immunoprecipitated by the respective YFP-tagged peptide labeled above. Images are representative of three independent experiments. The band size (30kDa) is labeled to the right of each blot.

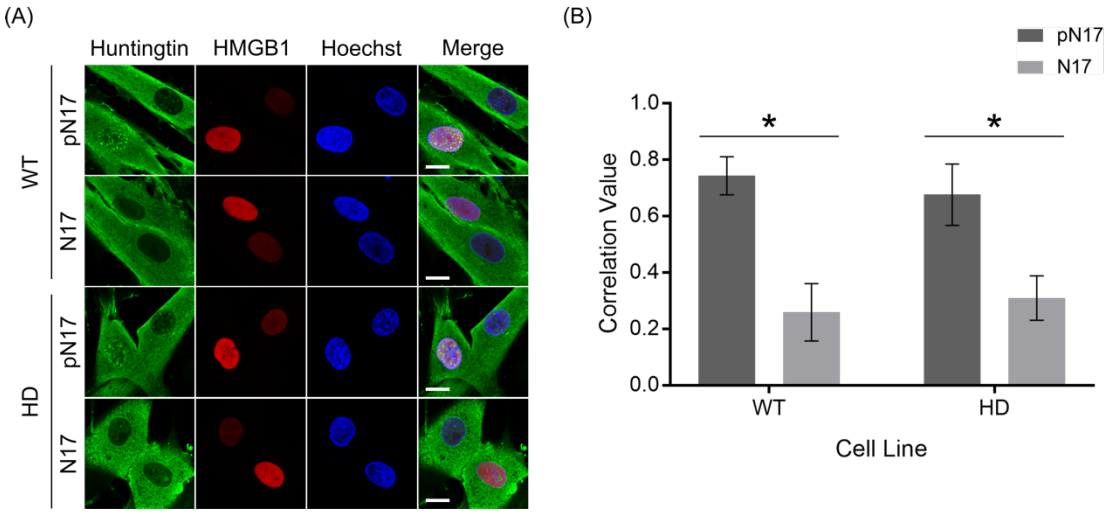

Figure 4: *Visualization and quantification of the correlation between huntingtin and HMGB1 localization.* (A) Anti-pN17 or anti-N17 and anti-HMGB1 antibodies were co-stained in hTERT-immortalized TruHD-Q21Q18 (WT) and TruHD-Q43Q17 (HD) human fibroblasts. Greater nuclear phospho-huntingtin (red channel) is seen when there is greater nuclear HMGB1 fluorescence (green channel), while less nuclear phospho-huntingtin is seen with less nuclear HMGB1. This correlative relationship can be observed in both WT and HD lines using the anti-pN17 antibody, but is not seen in cells stained with anti-N17. Images were captured using confocal microscopy at 60X magnification with an oil-immersion lens. Scale bar is 10µm. (B) The correlation of nuclear huntingtin and HMGB1 was quantified using Pearson correlation and computed using a Python script written on PyCharm CE 2016.1.2. An average correlation value of 0.744 for WT and 0.677 for HD represents a very strong correlation between pN17 and HMGB1 (dark gray bars). Correlation values for N17 and HMGB1 were 0.260 for WT and 0.310 for HD, indicating a weak relationship (light gray bars). >500 cells were captured and measured. *P-values < 0.01 at n = 3.

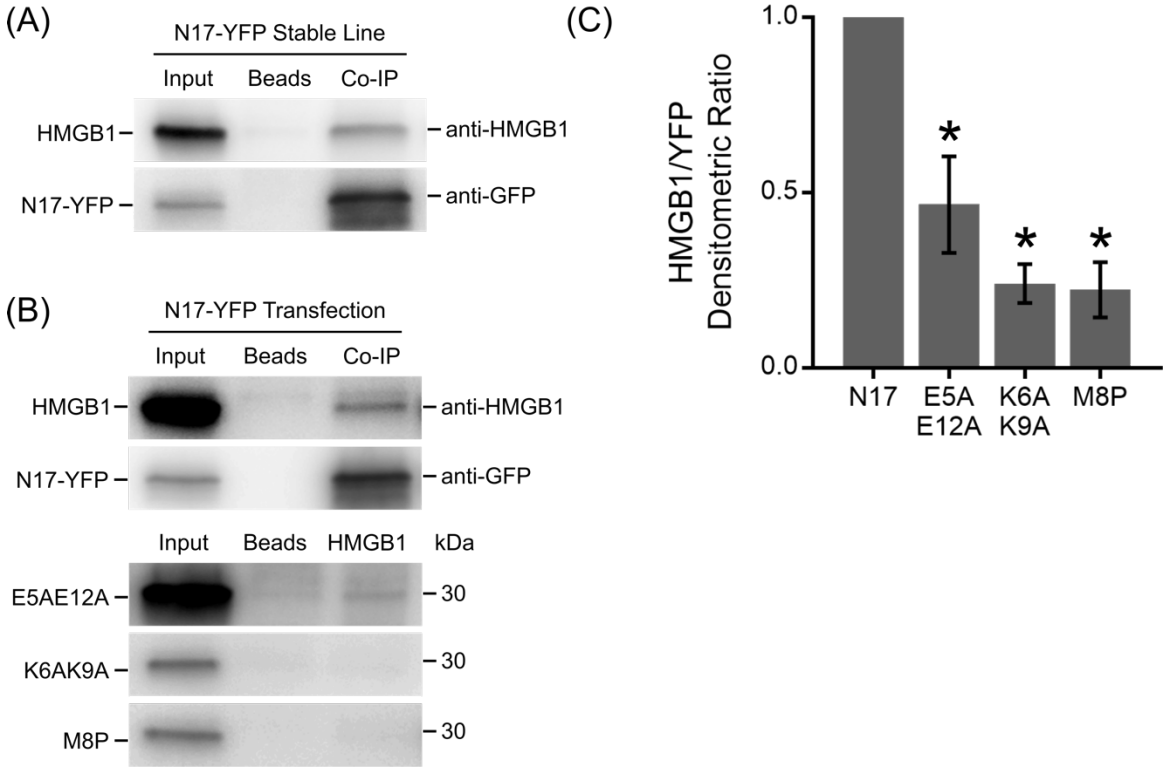

Figure 5: *HMGB1 co-immunoprecipitated with the N17 domain.* (A) ST*Hdh*$^{Q7/Q7}$ cells stably expressing N17-YFP and (B) ST*Hdh*$^{Q7/Q7}$ cells transfected with N17-YFP and mutants N17 E5AE12A-YFP, N17 K6AK9A-YFP, and N17 M8P-YFP were used for Co-IP. Lysates were incubated in protein A agarose beads with or without the YFP-specific antibody, anti-GFP. Co-IP products were separated by SDS-PAGE and immunoblotted with anti-HMGB1 and anti-GFP to detect the YFP tag of each peptide. The "Input" lane represents the positive control, the "Beads" lane represents the negative control, and the "Co-IP" lane indicates the presence of the respective protein written to the left of each blot. The "HMGB1" lane in (B) indicates the presence of HMGB1 pulled down by the respective YFP-tagged peptides labeled to the left of each blot. Images are representative of three independent experiments. (C) Protein levels were quantified for wild-type N17 and mutants E5AE12A, K6AK9A, and M8P. The pixel density of each band was calculated and normalized to wild-type N17. Error bars represent standard error. *P-values < 0.01 at n = 3.

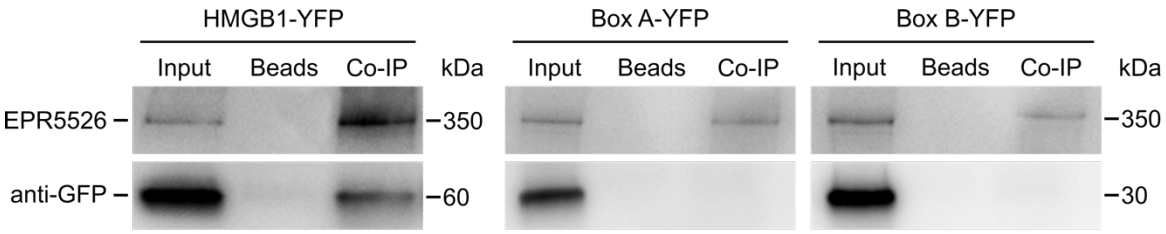

Figure 6: *Huntingtin interacts with full-length HMGB1, but not its individual boxes.* ST*Hdh*$^{Q7/Q7}$ cells were harvested to Co-IP overexpressed HMGB1-YFP, box A-YFP, and box B-YFP using huntingtin-specific antibody, EPR5526. The presence of HMGB1 and the absence of box A and B under the Co-IP lanes indicate that huntingtin interacts with full-length HMGB1, but not its individual boxes. The "Input" lane represents the positive control, the "Beads" lane represents the negative control, and the "Co-IP" lane indicates the presence of the respective YFP-tagged protein or fragment labeled above each blot.

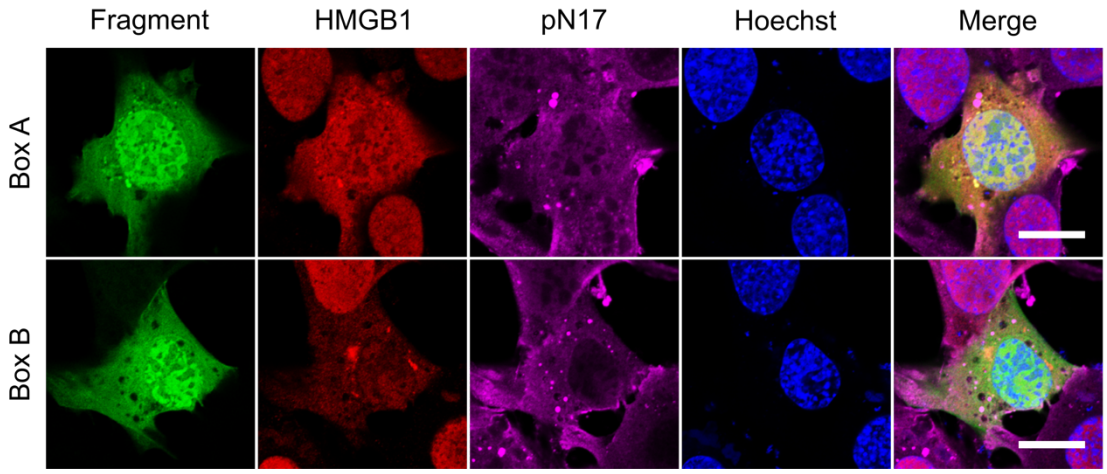

Figure 7: *Overexpression of HMGB1 boxes promotes cytoplasmic targeting of endogenous HMGB1.* ST*Hdh*$^{Q7/Q7}$ cells were transfected with either box A-YFP or box B-YFP, and stained using anti-HMGB1 and anti-pN17. Both boxes localize diffusely throughout the cell, but are predominantly nuclear (green channel), HMGB1 fluorescence is evenly distributed throughout the whole cell (red channel), and phospho-huntingtin is cytoplasmic (magenta channel). Nuclear Hoechst stain is represented by the blue channel, and a merged image is present as the far right channel. Images were acquired using confocal microscopy at 60X magnification with an oil-immersion lens. Scale bar is 10µm.

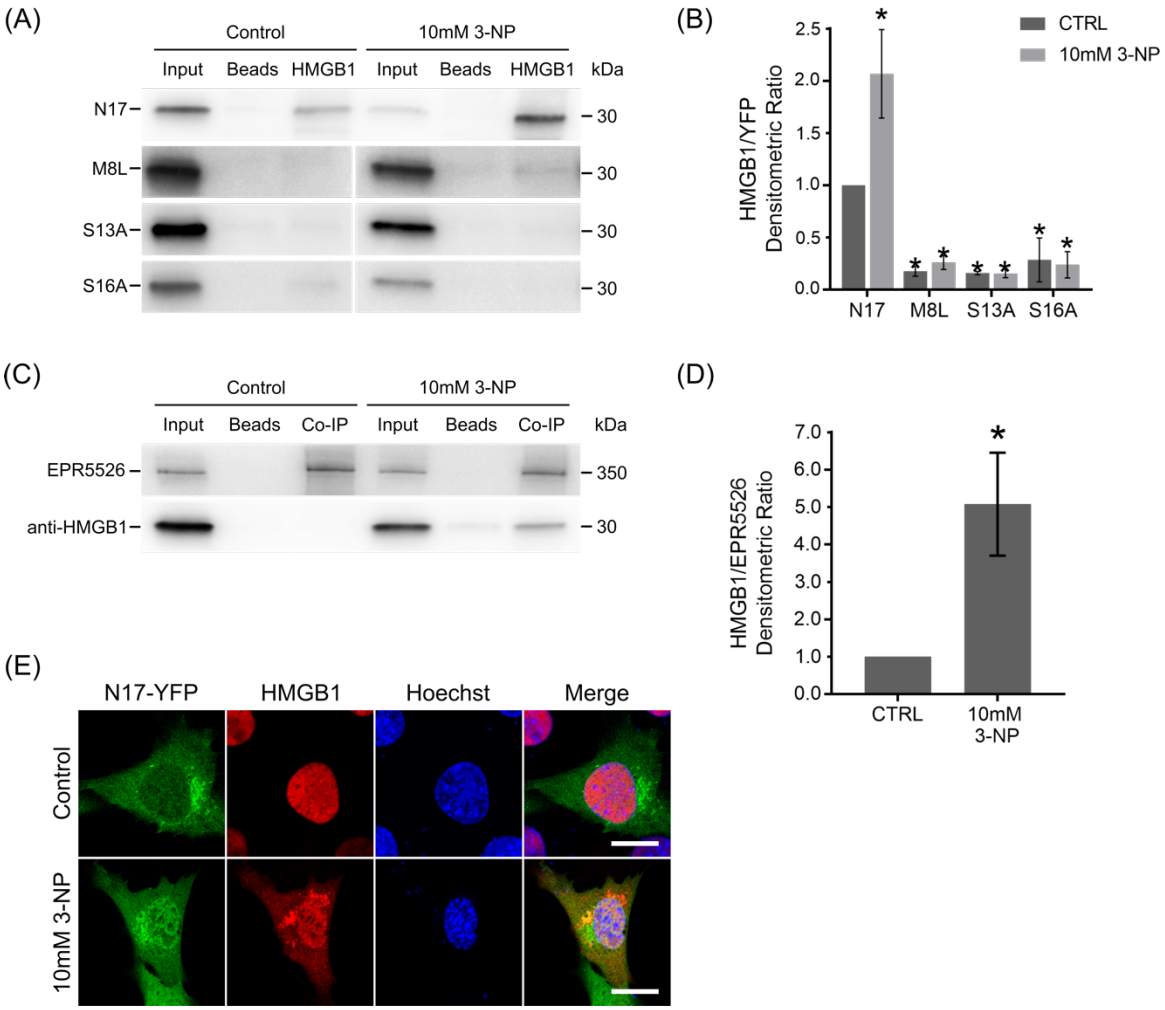

Figure 8: *The interaction between HMGB1 and huntingtin increases with oxidative stress.* (A) ST*Hdh*$^{Q7/Q7}$ cells were treated with or without 10mM 3-NP for 1.5h for the Co-IP of HMGB1 using overexpressed wild-type N17-YFP or one of its three mutants: N17 M8L-YFP, N17 S13A-YFP, and N17 S16A-YFP. Lysates were incubated in protein A agarose beads with or without anti-GFP, in blot (A) and with or without EPR5526, in blot (C). Western blots were immunoblotted with anti-HMGB1. The "Input" lane represents the positive control, the "Beads" lane represents the negative control, and the "HMGB1" lane indicates the presence of HMGB1 pulled down by the respective YFP-tagged peptides labeled to the left of each blot. (B) Protein levels were quantified for wild-type N17 and mutants M8L, S13A, and S16A with or without 3-NP treatment. The pixel density of each Co-IP band was calculated and normalized to wild-type N17 control (without treatment). Error bars represent standard error. All mutants and treatment conditions were significantly different from the control; however, no significant

difference was noted between treatment conditions of each N17 mutant. *P-value <0.01 at n = 3. (C) ST*Hdh*$^{Q7/Q7}$ cells were cultured and prepared similar to (A) to Co-IP endogenous HMGB1 using EPR5526. The "Co-IP" lane indicates the presence of the respective protein written to the left of each blot. (D) The same quantification methods were used as (B) *P-value <0.01 at n = 3. (E) ST*Hdh*$^{Q7/Q7}$ cells were transfected with N17-YFP (green channel) and probed with anti-HMGB1 (red channel). With the addition of 10mM 3-NP, we observed that N17-YFP localizes to the nucleus and HMGB1 targets the cytoplasm. However, nuclear levels of HMGB1 are still present. Images were acquired using confocal microscopy at 60X magnification with an oil-immersion lens. Scale bar is 10µm.

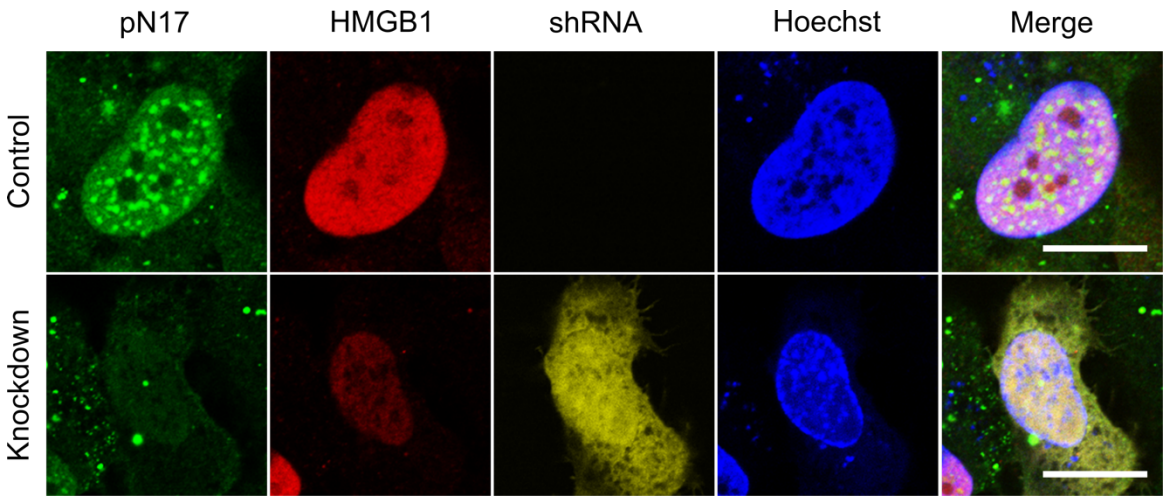

Figure 9: *HMGB1 knockdown abrogates nuclear entry of phospho-huntingtin.* RPE1 cells were transfected with a human HMGB1 shRNA to reduce intracellular HMGB1 levels and then stained with anti-HMGB1 and anti-pN17. Upon HMGB1 knockdown (red channel), nuclear fluorescence of pN17 was dramatically reduced (green channel). The HMGB1 shRNA is tagged with a GFP fluorophore, which is a marker to confirm successful transfection of the shRNA into cells (yellow channel). Images are representative of >100 independent cells. Confocal microscopy was used to acquire these images. An oil-immersion 60X lens was used. Scale bar is 10µm.

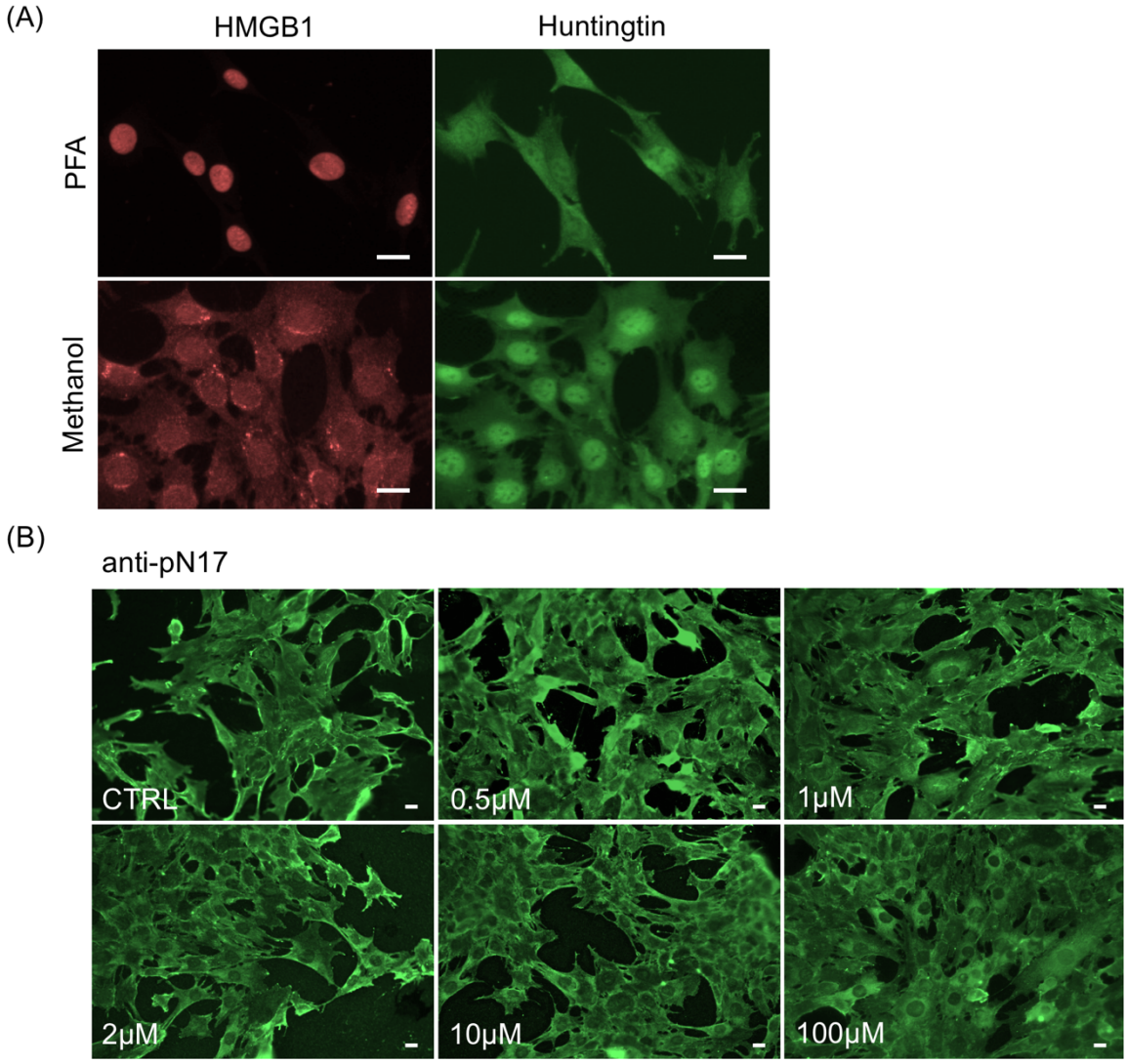

Figure 10: *Huntingtin localization in the presence of glycyrrhizic acid.* (A) ST*Hdh*$^{Q7/Q7}$ cells were used to test the effects of staining patterns after employing different fixation methods. Methanol fixation highlights HMGB1 in the cytoplasm, particularly in the ER, which is atypical compared to what is commonly reported. Conversely, paraformaldehyde (PFA) fixation detects endogenous HMGB1 in the nucleus, which is its characterized phenotype, thus PFA fixation was used for all subsequent experiments involving HMGB1. Images were taken on an inverted immunofluorescence microscope at 20X magnification. Scale bar is 10μm. (B) ST*Hdh*$^{Q7/Q7}$ cells were treated with GA at concentrations of 0.5, 1, 2, 10, and 100μM for 24h before methanol fixation and staining of the anti-pN17 antibody was conducted. Observations suggest that huntingtin remains cytoplasmic regardless of GA concentration. Images were taken on an inverted immunofluorescence microscope at 20X magnification. Scale bar is 10μm.

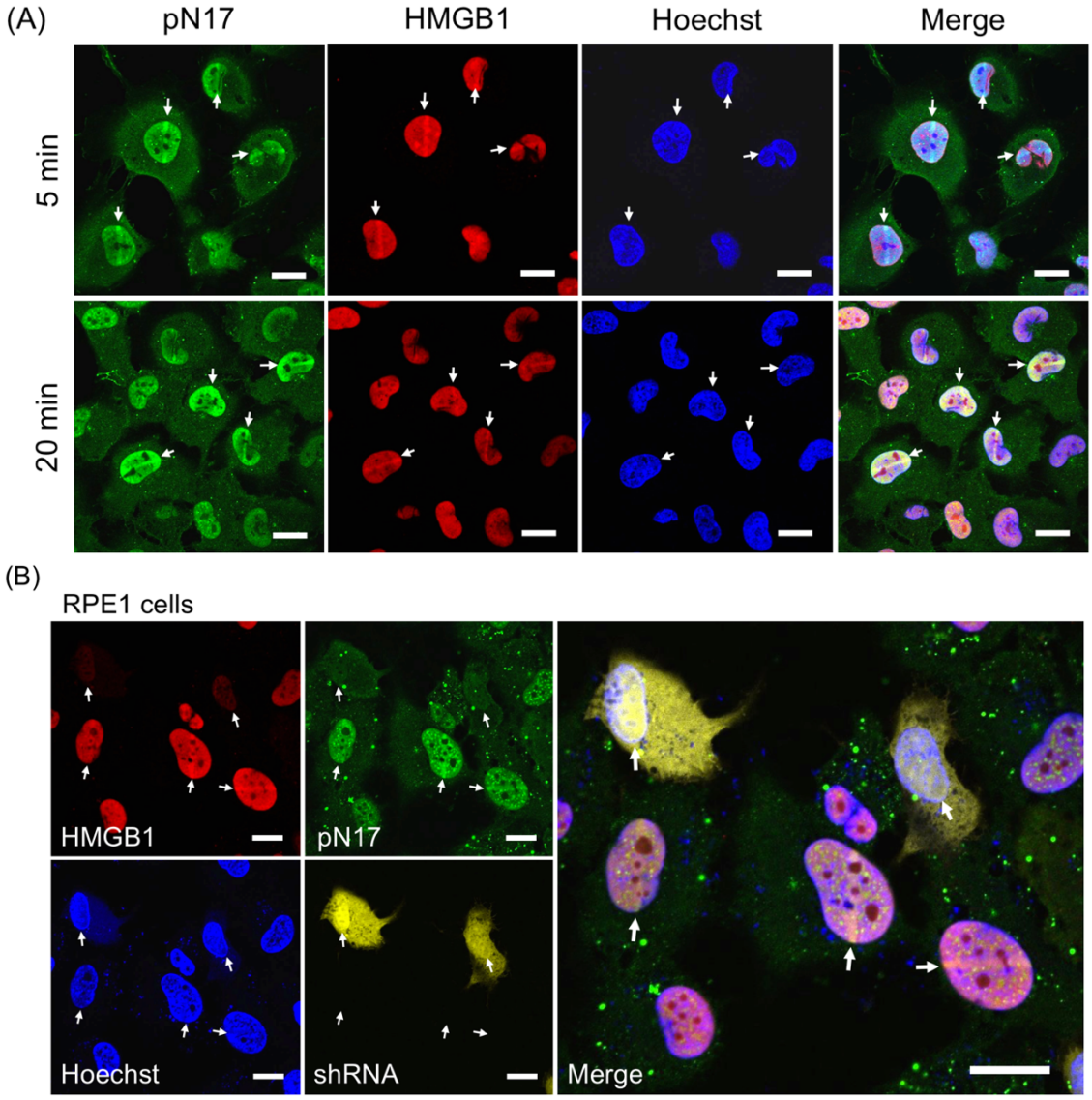

Figure 11: *Localization of phosphorylated huntingtin and HMGB1 to sites of DNA damage via laser stripe assay.* (A) A 405nm laser was used to induce DNA damage. RPE1 cells were incubated for 5 and 20 min prior to fixation with 4% PFA. After treatment, cells were probed using anti-pN17 (green channel) and anti-HMGB1 (red channel). Both proteins localized to the stripe, indicating that they may be interacting at sites of DNA damage. White arrows point to the location of the laser stripe. (B) The same procedure was conducted as in (A) except for the addition of an HMGB1 shRNA via transfection to knockdown HMGB1 prior to irradiation. The shRNA channel represents the GFP marker used to indicate the successful transfection of the shRNA (yellow channel). White arrows point to the location of the laser stripe. Confocal microscopy was used to acquire these images. An oil-immersion 60X lens was used. Scale bar is 10µm.

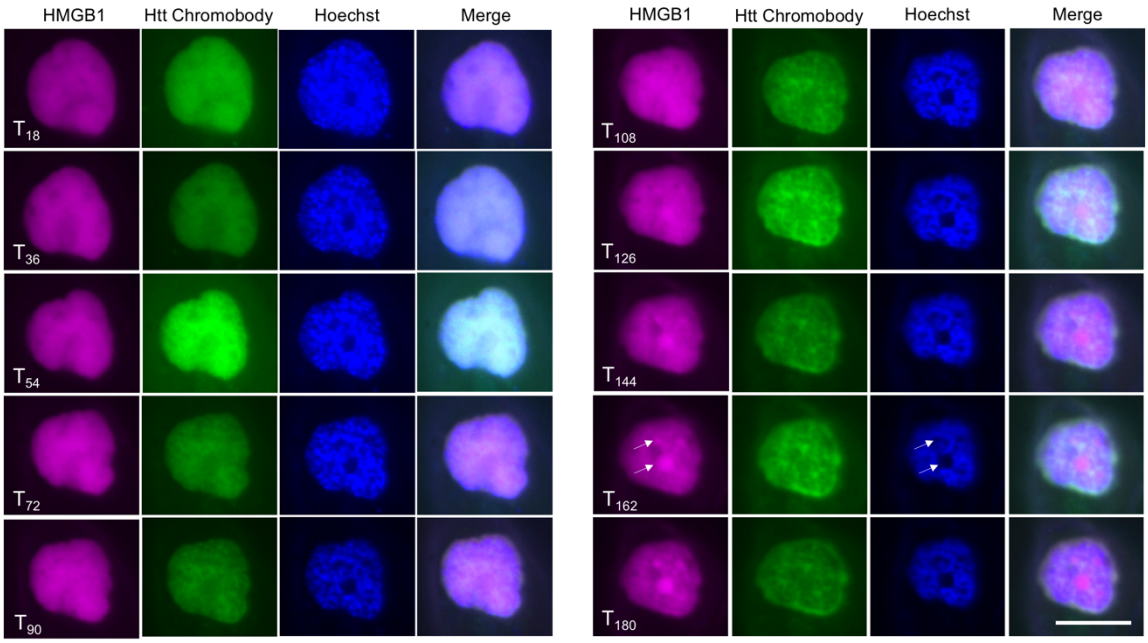

Figure 12: *The localization of HMGB1 to sites of euchromatin.* A 3h 40mM $KBrO_3$ treatment of RPE1 cells overexpressing mCh-HMGB1 (magenta channel) and the huntingtin (Htt) chromobody (green channel) was captured using live cell imaging. At ~T_{126} HMGB1 (magenta channel) begins to localize to nuclear "holes" (represented by areas unstained by Hoechst 33342; blue channel) indicated by white arrows. At ~T_{90} huntingtin chromobodies begin to form punctate clusters within the nucleus. Their identity is unknown as they are unlike the bright and circular phospho-huntingtin puncta that are regularly observed. Almost no co-localization of mCh-HMGB1 with these punctate regions formed by the huntingtin chromobody can be detected. A widefield microscope was used and imaged under an oil-immersion 60X magnification. Scale bar is 10µm.

REFERENCES

1. Huntingtin,G. (1965) George Huntington (1850-1916) and hereditary chorea. *JAMA*, **193**, 680.

2. Harper,P.S. (1996) Huntington's disease. *The Royal Society*, **354**, 957-961.

3. Myers,R.H. (2004) Huntington's disease genetics. *Neurotherapeutics*, **1**, 255–262.

4. Watt,D.C. and Seller,A. (1993) A Clinico-Genetic Study of Psychiatric Disorder in Huntington's Chorea Cambridge University Press.

5. Abildtrup,M. and Shattock,M. (2013) Cardiac Dysautonomia in Huntington's Disease. *J. Huntingtons Dis.*, **2**, 251–261.

6. Lanska,D.J., Lavine,L., Lanska,M.J. and Schoenberg,B.S. (1988) Huntington's disease mortality in the United States. *Neurology*, **38**, 769–769.

7. Nance,M.A. and Myers,R.H. (2001) Juvenile onset Huntington's disease?clinical and research perspectives. *Ment. Retard. Dev. Disabil. Res. Rev.*, **7**, 153–157.

8. Graveland,G., Williams,R. and DiFiglia,M. (1985) Evidence for degenerative and regenerative changes in neostriatal spiny neurons in Huntington's disease. *Science*, **227**, 770–773.

9. Vonsattel,J.-P., Myers,R.H., Stevens,T.J., Ferrante,R.J., Bird,E.D. and Richardson,E.P. (1985) Neuropathological Classification of Huntington's Disease. *J. Neuropathol. Exp. Neurol.*, **44**, 559–577.

10. de la Monte,S.M., Vonsattel,J.-P. and Richardson,E.P. (1988) Morphometric Demonstration of Atrophic Changes in the Cerebral Cortex, White Matter, and Neostriatum in Huntington's Disease. *J. Neuropathol. Exp. Neurol.*, **47**, 516–525.

11. Arsalidou,M., Duerden,E.G. and Taylor,M.J. (2013) The centre of the brain: topographical model of motor, cognitive, affective, and somatosensory functions of the basal ganglia. *Hum. Brain Mapp.*, **34**, 3031–3054.

12. Gusella,J.F., Wexler,N.S., Michael Conneally,P., Naylor,S.L., Anderson,M.A., Tanzi,R.E., Watkins,P.C., Ottina,K., Wallace,M.R., Sakaguchi,A.Y., *et al.* (1983) A polymorphic DNA marker genetically linked to Huntington's disease. *Nature*, **306**, 234–238.

13. Stine,O.C., Pleasant,N., Franz,M.L., Abbott,M.H., Folstein,S.E. and Ross,C.A. (1993) Correlation between the onset age of Huntington's disease and length of the trinucleotide repeat in IT-15. *Hum. Mol. Genet.*, **2**, 1547–1549.

14. McNeil,S.M., Novelletto,A., Srinidhi,J., Barnes,G., Kornbluth,I., Altherr,M.R., Wasmuth,J.J., Gusella,J.F., MacDonald,M.E. and Myers,R.H. (1997) Reduced Penetrance of the Huntington's Disease Mutation. *Hum. Mol. Genet.*, **6**, 775–779.

15. Andrew,S.E., Paul Goldberg,Y., Kremer,B., Telenius,H., Theilmann,J., Adam,S., Starr,E., Squitieri,F., Lin,B., Kalchman,M.A., *et al.* (1993) The relationship between trinucleotide (CAG) repeat length and clinical features of Huntington's disease. *Nat. Genet.*, **4**, 398–403.

16. Kearney,J.A. (2011) Genetic modifiers of neurological disease. *Curr. Opin. Genet. Dev.*, **21**, 349–353.

17. van Dellen,A., Grote,H.E. and Hannan,A.J. (2005) Gene-environment interactions, neuronal dysfunction and pathological plasticity in Huntington's disease. *Clinical and Experimental Pharmacology and Physiology*, **32**, 1007–1019.

18. Sharp,A.H., Loev,S.J., Schilling,G., Li,S.-H., Li,X.-J., Bao,J., Wagster,M.V., Kotzuk,J.A., Steiner,J.P., Lo,A., *et al.* (1995) Widespread expression of Huntington's disease gene (IT15) protein product. *Neuron*, **14**, 1065–1074.

19. Andrade,M.A., Petosa,C., O'Donoghue,S.I., Müller,C.W. and Bork,P. (2001) Comparison of ARM and HEAT protein repeats. *J. Mol. Biol.*, **309**, 1–18.

20. Kappel,C., Zachariae,U., Dölker,N. and Grubmüller,H. (2010) An unusual hydrophobic core confers extreme flexibility to HEAT repeat proteins. *Biophys. J.*, **99**, 1596–1603.

21. Groves,M.R., Hanlon,N., Turowski,P., Hemmings,B.A. and Barford,D. (1999) The structure of the protein phosphatase 2A PR65/A subunit reveals the conformation of its 15 tandemly repeated HEAT motifs. *Cell*, **96**, 99–110.

22. Atwal,R.S., Xia,J., Pinchev,D., Taylor,J., Epand,R.M. and Truant,R. (2007) Huntingtin has a membrane association signal that can modulate huntingtin aggregation, nuclear entry and toxicity. *Hum. Mol. Genet.*, **16**, 2600–2615.

23. Kim,M.W., Chelliah,Y., Kim,S.W., Otwinowski,Z. and Bezprozvanny,I. (2009) Secondary structure of Huntingtin amino-terminal region. *Structure*, **17**, 1205–1212.

24. Nagai,Y., Inui,T., Popiel,H.A., Fujikake,N., Hasegawa,K., Urade,Y., Goto,Y., Naiki,H. and Toda,T. (2007) A toxic monomeric conformer of the polyglutamine protein. *Nat. Struct. Mol. Biol.*, **14**, 332–340.

25. DiFiglia,M., Sapp,E., Chase,K., Schwarz,C., Meloni,A., Young,C., Martin,E., Vonsattel,J.P., Carraway,R. and Reeves,S.A. (1995) Huntingtin is a cytoplasmic protein associated with vesicles in human and rat brain neurons. *Neuron*, **14**, 1075–1081.

26. Velier,J., Kim,M., Schwarz,C., Kim,T.W., Sapp,E., Chase,K., Aronin,N. and DiFiglia,M. (1998) Wild-type and mutant huntingtins function in vesicle trafficking in the secretory and endocytic pathways. *Exp. Neurol.*, **152**, 34–40.

27. De Rooij,K. (1996) Subcellular localization of the Huntington's disease gene product in cell lines by immunofluorescence and biochemical subcellular fractionation. *Hum. Mol. Genet.*, **5**, 1093–1099.

28. Sari,Y. (2011) Huntington's Disease: From Mutant Huntingtin Protein to Neurotrophic Factor Therapy. *Int. J. Biomed. Sci.*, **7**, 89–100.

29. Desmond,C.R., Atwal,R.S., Xia,J. and Truant,R. (2012) Identification of a Karyopherin 1/ 2 Proline-Tyrosine Nuclear Localization Signal in Huntingtin Protein. *J. Biol. Chem.*, **287**, 39626–39633.

30. DiGiovanni,L.F., Mocle,A.J., Xia,J. and Truant,R. (2016) Huntingtin N17 domain is a reactive oxygen species sensor regulating huntingtin phosphorylation and localization. *Hum. Mol. Genet.*, **25**, 3937–3945.

31. Rockabrand,E., Slepko,N., Pantalone,A., Nukala,V.N., Kazantsev,A., Marsh,J.L., Sullivan,P.G., Steffan,J.S., Sensi,S.L. and Thompson,L.M. (2007) The first 17 amino acids of Huntingtin modulate its sub-cellular localization, aggregation and effects on calcium homeostasis. *Hum. Mol. Genet.*, **16**, 61–77.

32. Atwal,R.S., Desmond,C.R., Caron,N., Maiuri,T., Xia,J., Sipione,S. and Truant,R. (2011) Kinase inhibitors modulate huntingtin cell localization and toxicity. *Nat. Chem. Biol.*, **7**, 453–460.

33. Steffan,J.S. (2004) SUMO Modification of Huntingtin and Huntington's Disease Pathology. *Science*, **304**, 100–104.

34. Aiken,C.T., Steffan,J.S., Guerrero,C.M., Khashwji,H., Lukacsovich,T., Simmons,D., Purcell,J.M., Menhaji,K., Zhu,Y.-Z., Green,K., *et al.* (2009) Phosphorylation of threonine 3: implications for Huntingtin aggregation and neurotoxicity. *J. Biol. Chem.*, **284**, 29427–29436.

35. Gu,X., Greiner,E.R., Mishra,R., Kodali,R., Osmand,A., Finkbeiner,S., Steffan,J.S., Thompson,L.M., Wetzel,R. and Yang,X.W. (2009) Serines 13 and 16 are critical determinants of full-length human mutant huntingtin induced disease pathogenesis in HD mice. *Neuron*, **64**, 828–840.

36. Di Pardo,A., Maglione,V., Alpaugh,M., Horkey,M., Atwal,R.S., Sassone,J., Ciammola,A., Steffan,J.S., Fouad,K., Truant,R., *et al.* (2012) Ganglioside GM1 induces phosphorylation of mutant huntingtin and restores normal motor behavior in Huntington disease mice. *Proc. Natl. Acad. Sci. U. S. A.*, **109**, 3528–3533.

37. Maiuri,T., Woloshansky,T., Xia,J. and Truant,R. (2013) The huntingtin N17 domain is a multifunctional CRM1 and Ran-dependent nuclear and cilial export signal. *Hum. Mol. Genet.*, **22**, 1383–1394.

38. Caron,N.S., Desmond,C.R., Xia,J. and Truant,R. (2013) Polyglutamine domain flexibility mediates the proximity between flanking sequences in huntingtin. *Proceedings of the National Academy of Sciences*, **110**, 14610–14615.

39. Maiuri,T., Mocle,A.J., Hung,C.L., Xia,J., van Roon-Mom,W.M.C. and Truant,R. (2017) Huntingtin is a scaffolding protein in the ATM oxidative DNA damage response complex. *Hum. Mol. Genet.*, **26**, 395–406.

40. Feng,Z., Jin,S., Zupnick,A., Hoh,J., de Stanchina,E., Lowe,S., Prives,C. and Levine,A.J. (2006) p53 tumor suppressor protein regulates the levels of huntingtin gene expression. *Oncogene*, **25**, 1–7.

41. Shiloh,Y. and Ziv,Y. (2013) The ATM protein kinase: regulating the cellular response to genotoxic stress, and more. *Nat. Rev. Mol. Cell Biol.*, **14**, 197–210.

42. Guo,Z., Kozlov,S., Lavin,M.F., Person,M.D. and Paull,T.T. (2010) ATM activation by oxidative stress. *Science*, **330**, 517–521.

43. Kovtun,I.V., Liu,Y., Bjoras,M., Klungland,A., Wilson,S.H. and McMurray,C.T. (2007) OGG1 initiates age-dependent CAG trinucleotide expansion in somatic cells. *Nature*, **447**, 447–452.

44. Johns,E. (2012) The Chromosomal Proteins Elsevier.

45. Grosschedl,R., Giese,K. and Pagel,J. (1994) HMG domain proteins: architectural elements in the assembly of nucleoprotein structures. *Trends Genet.*, **10**, 94–100.

46. Liu,Y., Prasad,R. and Wilson,S.H. (2010) HMGB1: roles in base excision repair and related function. *Biochim. Biophys. Acta*, **1799**, 119–130.

47. Stros,M. (2010) HMGB proteins: interactions with DNA and chromatin. *Biochim. Biophys. Acta*, **1799**, 101–113.

48. Hardman,C.H., Broadhurst,R.W., Raine,A.R., Grasser,K.D., Thomas,J.O. and Laue,E.D. (1995) Structure of the A-domain of HMG1 and its interaction with DNA as studied by heteronuclear three- and four-dimensional NMR spectroscopy. *Biochemistry*, **34**, 16596–16607.

49. Weir,H.M., Kraulis,P.J., Hill,C.S., Raine,A.R., Laue,E.D. and Thomas,J.O. (1993) Structure of the HMG box motif in the B-domain of HMG1. *EMBO J.*, **12**, 1311–1319.

50. Read,C.M., Cary,P.D., Crane-Robinson,C., Driscoll,P.C. and Norman,D.G. (1993) Solution structure of a DNA-binding domain from HMG1. *Nucleic Acids Res.*, **21**, 3427–3436.

51. Bustin,M. (1999) Regulation of DNA-dependent activities by the functional motifs of the high-mobility-group chromosomal proteins. *Mol. Cell. Biol.*, **19**, 5237–5246.

52. Belgrano,F.S., de Abreu da Silva,I.C., Bastos de Oliveira,F.M., Fantappié,M.R. and Mohana-Borges,R. (2013) Role of the acidic tail of high mobility group protein B1 (HMGB1) in protein stability and DNA bending. *PLoS One*, **8**, e79572.

53. Martin,D.D.O., Ladha,S., Ehrnhoefer,D.E. and Hayden,M.R. (2015) Autophagy in Huntington disease and huntingtin in autophagy. *Trends Neurosci.*, **38**, 26–35.

54. Martinotti,S., Patrone,M. and Ranzato,E. (2015) Emerging roles for HMGB1 protein in immunity, inflammation, and cancer. *Immunotargets Ther*, **4**, 101–109.

55. Kim,J.-B., Sig Choi,J., Yu,Y.-M., Nam,K., Piao,C.-S., Kim,S.-W., Lee,M.-H., Han,P.-L., Park,J.-S. and Lee,J.-K. (2006) HMGB1, a novel cytokine-like mediator linking acute neuronal death and delayed neuroinflammation in the postischemic brain. *J. Neurosci.*, **26**, 6413–6421.

56. Lotze,M.T. and Tracey,K.J. (2005) High-mobility group box 1 protein (HMGB1): nuclear weapon in the immune arsenal. *Nat. Rev. Immunol.*, **5**, 331–342.

57. Tang,D., Kang,R., Zeh,H.J.,3rd and Lotze,M.T. (2010) High-mobility group box 1 and cancer. *Biochim. Biophys. Acta*, **1799**, 131–140.

58. Kang,R., Livesey,K.M., Zeh,H.J., Loze,M.T. and Tang,D. (2010) HMGB1: a novel Beclin 1-binding protein active in autophagy. *Autophagy*, **6**, 1209–1211.

59. Youn,J.H. and Shin,J.-S. (2006) Nucleocytoplasmic Shuttling of HMGB1 Is Regulated by Phosphorylation That Redirects It toward Secretion. *The Journal of Immunology*, **177**, 7889–7897.

60. Bonaldi,T., Talamo,F., Scaffidi,P., Ferrera,D., Porto,A., Bachi,A., Rubartelli,A., Agresti,A. and Bianchi,M.E. (2003) Monocytic cells hyperacetylate chromatin protein HMGB1 to redirect it towards secretion. *EMBO J.*, **22**, 5551–5560.

61. Bianchi,M., Beltrame,M. and Paonessa,G. (1989) Specific recognition of cruciform DNA by nuclear protein HMG1. *Science*, **243**, 1056–1059.

62. Pil,P.M., Chow,C.S. and Lippard,S.J. (1993) High-mobility-group 1 protein mediates DNA bending as determined by ring closures. *Proc. Natl. Acad. Sci. U. S. A.*, **90**, 9465–9469.

63. Bustin,M. and Reeves,R. (1996) High-mobility-group chromosomal proteins: architectural components that facilitate chromatin function. *Prog. Nucleic Acid Res. Mol. Biol.*, **54**, 35–100.

64. Muller,S., Ronfani,L. and Bianchi,M.E. (2004) Regulated expression and subcellular localization of HMGB1, a chromatin protein with a cytokine function. *J. Intern. Med.*, **255**, 332–343.

65. Prasad,R., Liu,Y., Deterding,L.J., Poltoratsky,V.P., Kedar,P.S., Horton,J.K., Kanno,S.-I., Asagoshi,K., Hou,E.W., Khodyreva,S.N., *et al.* (2007) HMGB1 is a cofactor in mammalian base excision repair. *Mol. Cell*, **27**, 829–841.

66. Kroemer,G., Mariño,G. and Levine,B. (2010) Autophagy and the Integrated Stress Response. *Mol. Cell*, **40**, 280–293.

67. Yang,Z. and Klionsky,D.J. (2010) Eaten alive: a history of macroautophagy. *Nat. Cell Biol.*, **12**, 814–822.

68. Hengartner,M.O. (2000) The biochemistry of apoptosis. *Nature*, **407**, 770–776.

69. Maiuri,M.C., Zalckvar,E., Kimchi,A. and Kroemer,G. (2007) Self-eating and self-killing: crosstalk between autophagy and apoptosis. *Nat. Rev. Mol. Cell Biol.*, **8**, 741–752.

70. Livesey,K.M., Kang,R., Vernon,P., Buchser,W., Loughran,P., Watkins,S.C., Zhang,L., Manfredi,J.J., Zeh,H.J.,3rd, Li,L., *et al.* (2012) p53/HMGB1 complexes regulate autophagy and apoptosis. *Cancer Res.*, **72**, 1996–2005.

71. Tang,D., Kang,R., Livesey,K.M., Cheh,C.-W., Farkas,A., Loughran,P., Hoppe,G., Bianchi,M.E., Tracey,K.J., Zeh,H.J.,3rd, *et al.* (2010) Endogenous HMGB1 regulates autophagy. *J. Cell Biol.*, **190**, 881–892.

72. Kang,R., Zeh,H.J., Lotze,M.T. and Tang,D. (2011) The Beclin 1 network regulates autophagy and apoptosis. *Cell Death Differ.*, **18**, 571–580.

73. Størmer,F.C., Reistad,R. and Alexander,J. (1993) Glycyrrhizic acid in liquorice--evaluation of health hazard. *Food Chem. Toxicol.*, **31**, 303–312.

74. Mollica,L., De Marchis,F., Spitaleri,A., Dallacosta,C., Pennacchini,D., Zamai,M., Agresti,A., Trisciuoglio,L., Musco,G. and Bianchi,M.E. (2007) Glycyrrhizin binds to high-mobility group box 1 protein and inhibits its cytokine activities. *Chem. Biol.*, **14**, 431–441.

75. Nishimoto,Y., Hisatsune,A., Katsuki,H., Miyata,T., Yokomizo,K. and Isohama,Y. (2010) Glycyrrhizin attenuates mucus production by inhibition of MUC5AC mRNA expression in vivo and in vitro. *J. Pharmacol. Sci.*, **113**, 76–83.

76. Li,W., Zhu,S., Li,J., Assa,A., Jundoria,A., Xu,J., Fan,S., Eissa,N.T., Tracey,K.J., Sama,A.E., *et al.* (2011) EGCG stimulates autophagy and reduces cytoplasmic HMGB1 levels in endotoxin-stimulated macrophages. *Biochem. Pharmacol.*, **81**, 1152–1163.

77. Tsung,A., Klune,J.R., Zhang,X., Jeyabalan,G., Cao,Z., Peng,X., Stolz,D.B., Geller,D.A., Rosengart,M.R. and Billiar,T.R. (2007) HMGB1 release induced by liver ischemia involves Toll-like receptor 4 dependent reactive oxygen species production and calcium-mediated signaling. *J. Exp. Med.*, **204**, 2913–2923.

78. Harja,E., Bu,D.-X., Hudson,B.I., Chang,J.S., Shen,X., Hallam,K., Kalea,A.Z., Lu,Y., Rosario,R.H., Oruganti,S., *et al.* (2008) Vascular and inflammatory stresses mediate atherosclerosis via RAGE and its ligands in apoE–/– mice. *J. Clin. Invest.*, **118**, 183–194.

79. Andrassy,M., Volz,H.C., Igwe,J.C., Funke,B., Eichberger,S.N., Kaya,Z., Buss,S., Autschbach,F., Pleger,S.T., Lukic,I.K., *et al.* (2008) High-mobility group box-1 in ischemia-reperfusion injury of the heart. *Circulation*, **117**, 3216–3226.

80. Musumeci,D., Roviello,G.N. and Montesarchio,D. (2014) An overview on HMGB1 inhibitors as potential therapeutic agents in HMGB1-related pathologies. *Pharmacol. Ther.*, **141**, 347–357.

81. Ehrnhoefer,D.E. (2006) Green tea (-)-epigallocatechin-gallate modulates early events in huntingtin misfolding and reduces toxicity in Huntington's disease models. *Hum. Mol. Genet.*, **15**, 2743–2751.

82. Shen,J.-L., Chen,Y.-S., Lin,J.-Y., Tien,Y.-C., Peng,W.-H., Kuo,C.-H., Tzang,B.-S., Wang,H.-L., Tsai,F.-J., Chou,M.-C., *et al.* (2011) Neuron Regeneration and Proliferation Effects of Danshen and Tanshinone IIA. *Evid. Based. Complement. Alternat. Med.*, **2011**, 378907.

83. Li,W., Li,J., Ashok,M., Wu,R., Chen,D., Yang,L., Yang,H., Tracey,K.J., Wang,P., Sama,A.E., *et al.* (2007) A cardiovascular drug rescues mice from lethal sepsis by selectively attenuating a late-acting proinflammatory mediator, high mobility group box 1. *J. Immunol.*, **178**, 3856–3864.

84. Fink,M.P. (2008) Ethyl pyruvate. *Curr. Opin. Anaesthesiol.*, **21**, 160–167.

85. Davé,S.H., Tilstra,J.S., Matsuoka,K., Li,F., DeMarco,R.A., Beer-Stolz,D., Sepulveda,A.R., Fink,M.P., Lotze,M.T. and Plevy,S.E. (2009) Ethyl pyruvate decreases HMGB1 release and ameliorates murine colitis. *J. Leukoc. Biol.*, **86**, 633–643.

86. Li,M.-L., Wang,X.-F., Tan,Z.-J., Dong,P., Gu,J., Lu,J.-H., Wu,X.-S., Zhang,L., Ding,Q.-C., Wu,W.-G., *et al.* (2012) Ethyl Pyruvate Administration Suppresses Growth and Invasion of Gallbladder Cancer Cells via Downregulation of Hmgb1-Rage Axis. *Int. J. Immunopathol. Pharmacol.*, **25**, 955–965.

87. Jang,M., Lee,M.J. and Cho,I.-H. (2014) Ethyl pyruvate ameliorates 3-nitropropionic acid-induced striatal toxicity through anti-neuronal cell death and anti-inflammatory mechanisms. *Brain Behav. Immun.*, **38**, 151–165.

88. Wang,H., Ward,M.F. and Sama,A.E. (2014) Targeting HMGB1 in the treatment of sepsis. *Expert Opin. Ther. Targets*, **18**, 257–268.

89. Gnanasekar,M., Kalyanasundaram,R., Zheng,G., Chen,A., Bosland,M.C. and Kajdacsy-Balla,A. (2013) HMGB1: A Promising Therapeutic Target for Prostate Cancer. *Prostate Cancer*, **2013**, 157103.

90. Nguyen,A.H., Detty,S.Q. and Agrawal,D.K. (2017) Clinical Implications of High-mobility Group Box-1 (HMGB1) and the Receptor for Advanced Glycation End-products (RAGE) in Cutaneous Malignancy: A Systematic Review. *Anticancer Res.*, **37**, 1–7.

91. Pilzweger,C. and Holdenrieder,S. (2015) Circulating HMGB1 and RAGE as Clinical Biomarkers in Malignant and Autoimmune Diseases. *Diagnostics (Basel)*, **5**, 219–253.

92. Li,W., Sama,A. and Wang,H. (2006) Role of HMGB1 in cardiovascular diseases. *Curr. Opin. Pharmacol.*, **6**, 130–135.

93. Rajaram,S., Pavie,B., Wu,L.F. and Altschuler,S.J. (2012) PhenoRipper: software for rapidly profiling microscopy images. *Nat. Methods*, **9**, 635–637.

94. Desmond,C.R., Atwal,R.S., Xia,J. and Truant,R. (2012) Identification of a karyopherin β1/β2 proline-tyrosine nuclear localization signal in huntingtin protein. *J. Biol. Chem.*, **287**, 39626–39633.

95. Brouillet,E. (2014) The 3-NP Model of Striatal Neurodegeneration. *Curr. Protoc. Neurosci.*, **67**, 9.48.1–14.

96. Tang,D., Kang,R., Zeh,H.J. and Lotze,M.T. (2011) High-Mobility Group Box 1, Oxidative Stress, and Disease. *Antioxid. Redox Signal.*, **14**, 1315–1335.

97. Brázda,V., Laister,R.C., Jagelská,E.B. and Arrowsmith,C. (2011) Cruciform structures are a common DNA feature important for regulating biological processes. *BMC Mol. Biol.*, **12**, 33.

98. Dintilhac,A. and Bernués,J. (2002) HMGB1 interacts with many apparently unrelated proteins by recognizing short amino acid sequences. *J. Biol. Chem.*, **277**, 7021–7028.

99. Calogero,S., Grassi,F., Aguzzi,A., Voigtländer,T., Ferrier,P., Ferrari,S. and Bianchi,M.E. (1999) The lack of chromosomal protein Hmg1 does not disrupt cell growth but causes lethal hypoglycaemia in newborn mice. *Nat. Genet.*, **22**, 276–280.

100. Yang,H., Antoine,D.J., Andersson,U. and Tracey,K.J. (2013) The many faces of HMGB1: molecular structure-functional activity in inflammation, apoptosis, and chemotaxis. *J. Leukoc. Biol.*, **93**, 865–873.

101. Murugesapillai,D., McCauley,M.J., James Maher,L. and Williams,M.C. (2016) Single-molecule studies of high-mobility group B architectural DNA bending proteins. *Biophys. Rev.*, **9**, 17–40.

102. Shin,Y.-J., Kim,M.-S., Kim,M.-S., Lee,J., Kang,M. and Jeong,J.-H. (2013) High-mobility group box 2 (HMGB2) modulates radioresponse and is downregulated by p53 in colorectal cancer cell. *Cancer Biol. Ther.*, **14**, 213–221.

103. Ronfani,L., Ferraguti,M., Croci,L., Ovitt,C.E., Schöler,H.R., Consalez,G.G. and Bianchi,M.E. (2001) Reduced fertility and spermatogenesis defects in mice lacking chromosomal protein Hmgb2. *Development*, **128**, 1265–1273.

104. Yamoah,K., Brebene,A., Baliram,R., Inagaki,K., Dolios,G., Arabi,A., Majeed,R., Amano,H., Wang,R., Yanagisawa,R., *et al.* (2008) High-Mobility Group Box Proteins Modulate Tumor Necrosis Factor-α Expression in Osteoclastogenesis via a Novel Deoxyribonucleic Acid Sequence. *Mol. Endocrinol.*, **22**, 1141–1153.

105. Kosugi,S., Hasebe,M., Tomita,M. and Yanagawa,H. (2008) Nuclear export signal consensus sequences defined using a localization-based yeast selection system. *Traffic*, **9**, 2053–2062.

106. Zappavigna,V., Falciola,L., Helmer-Citterich,M., Mavilio,F. and Bianchi,M.E. (1996) HMG1 interacts with HOX proteins and enhances their DNA binding and transcriptional activation. *EMBO J.*, **15**, 4981–4991.

107. Rowell,J.P., Simpson,K.L., Stott,K., Watson,M. and Thomas,J.O. (2012) HMGB1-facilitated p53 DNA binding occurs via HMG-Box/p53 transactivation domain interaction, regulated by the acidic tail. *Structure*, **20**, 2014–2024.

108. Steffan,J.S., Kazantsev,A., Spasic-Boskovic,O., Greenwald,M., Zhu,Y.-Z., Gohler,H., Wanker,E.E., Bates,G.P., Housman,D.E. and Thompson,L.M. (2000) The Huntington's disease protein interacts with p53 and CREB-binding protein and represses transcription. *Proceedings of the National Academy of Sciences*, **97**, 6763–6768.

109. Plomann,M., Lange,R., Vopper,G., Cremer,H., Heinlein,U.A.O., Scheff,S., Baldwin,S.A., Leitges,M., Cramer,M., Paulsson,M., *et al.* (1998) PACSIN, a brain protein that is upregulated upon differentiation into neuronal cells. *Eur. J. Biochem.*, **256**, 201–211.

110. Pérez-Otaño,I., Luján,R., Tavalin,S.J., Plomann,M., Modregger,J., Liu,X.-B., Jones,E.G., Heinemann,S.F., Lo,D.C. and Ehlers,M.D. (2006) Endocytosis and synaptic removal of NR3A-containing NMDA receptors by PACSIN1/syndapin1. *Nat. Neurosci.*, **9**, 611–621.

111. Schael,S., Nüchel,J., Müller,S., Petermann,P., Kormann,J., Pérez-Otaño,I., Martínez,S.M., Paulsson,M. and Plomann,M. (2013) Casein kinase 2 phosphorylation of protein kinase C and casein kinase 2 substrate in neurons (PACSIN) 1 protein regulates neuronal spine formation. *J. Biol. Chem.*, **288**, 9303–9312.

112. Qi,M.-L., Tagawa,K., Enokido,Y., Yoshimura,N., Wada,Y.-I., Watase,K., Ishiura,S.-I., Kanazawa,I., Botas,J., Saitoe,M., *et al.* (2007) Proteome analysis of soluble nuclear proteins reveals that HMGB1/2 suppress genotoxic stress in polyglutamine diseases. *Nat. Cell Biol.*, **9**, 402–414.

113. van der Meer,B.W., Coker,G. and Chen,S.-Y.S. (1994) Resonance energy transfer: theory and data Wiley-VCH.

114. Margineanu,A., Chan,J.J., Kelly,D.J., Warren,S.C., Flatters,D., Kumar,S., Katan,M., Dunsby,C.W. and French,P.M.W. (2016) Screening for protein-protein interactions using Förster resonance energy transfer (FRET) and fluorescence lifetime imaging microscopy (FLIM). *Sci. Rep.*, **6**, 28186.

115. Jang,B.-C., Muñoz-Najar,U., Paik,J.-H., Claffey,K., Yoshida,M. and Hla,T. (2003) Leptomycin B, an inhibitor of the nuclear export receptor CRM1, inhibits COX-2 expression. *J. Biol. Chem.*, **278**, 2773–2776.

116. Chook,Y.M. and Süel,K.E. (2011) Nuclear import by karyopherin-βs: recognition and inhibition. *Biochim. Biophys. Acta*, **1813**, 1593–1606.